Hindawi
Shock and Vibration
Volume 2019, Article ID 3261628, 20 pages
https://doi.org/10.1155/2019/3261628

Research Article

Creating Nodes at Selected Locations in a Harmonically Excited Structure Using Feedback Control and Green's Function

Bassam A. Albassam

King Saud University, College of Engineering, Mechanical Engineering Department, Box 800, Riyadh 11421, Saudi Arabia

Correspondence should be addressed to Bassam A. Albassam; albassam@ksu.edu.sa

Received 22 May 2018; Revised 20 December 2018; Accepted 19 January 2019; Published 7 February 2019

Academic Editor: Chengzhi Shi

The paper deals with designing a control force to create nodal point(s) having zero displacements and/or zero slopes at selected locations in a harmonically excited vibrating structure. It is shown that the steady-state vibrations at desired points can be eliminated using feedback control forces. These control forces are constructed from displacement and/or velocity measurements using sensors located either at the control force position or at some other locations. Dynamic Green's function is exploited to derive a simple and exact closed from expression for the control force. Under a certain condition, this control force can be generated using passive elements such as springs and dampers. Numerical examples demonstrate the applicability of the method in various cases.

1. Introduction

In recent years, there has been a considerable interest in modeling and controlling flexible structures. This is due to the use of lightweight materials for the purposes of speed and fuel efficiency. These structures are characterized by low internal damping leading to prolonged vibrations, resulting in problems such as human discomfort, component failure, performance degradation, noise, and many other problems. Moreover, the performance is substantially degraded in some structures that are equipped with sensitive elements due to the occurrence of vibration. Therefore, it is desirable to eliminate the vibration from a certain part of the structure more than the other. For example, large flexible space structures are usually built from lightweight materials having low damping. Any excitation can cause vibrations that may propagate throughout the whole structure. In such a case, it is desirable to confine the vibrations in some chosen insensitive part while keeping other parts, for instance, an extremely sensitive antenna, relatively undisturbed.

There are a number of ways in which the vibration in a flexible structure can be eliminated or minimized. The first approach is to reduce or eliminate the external disturbance that excites the structure. Although this is always the preferred counter measure, but in many cases, there is little that can be done to change the nature of the driving force. The second approach is to modify the system to avoid vibrations, especially, during resonance. This may entail significant design, and it may be difficult to be applied for existing structures. A third applicable approach is to apply one of the vibration control approaches that can either absorb the vibrational energy or load transmission path for the disturbing vibration. In conventional terminology, passive, active, hybrid, and semiactive are listed in the literature as four common classifications of vibration control methods. Passive control involves some form of structural modification or redesign, often including the use of springs and dampers that leads to the mitigation of vibrations. An active control scheme augments the structure with sensors, actuators, and some form of an electronic control system to generate active force that can be controlled with different algorithms to make the system more responsive to disturbances. The hybrid approach is a combination of active and passive ones intended to reduce the amount of external power necessary to achieve system control in comparison

with the potentially large control effort required in the active scheme. The semiactive (also known as adaptive-passive) method integrates tuning control schemes with tunable passive devices by replacing the active force generators with modulated variable components such as variable rate damping and stiffness elements.

There is a wealth of literature dealing with vibration control using the aforementioned approaches in the form of an vibration absorber, which is a device originally invented by Frahm [1]. He has registered a US patent in 1909 for "Device of Damping Vibrations of Bodies." The first mathematical theory for a dynamic vibration absorber (DVA) was presented by Ormondroyd and Den Hartog [2]. Later, Brock [3] derived an analytical expression for the optimal damping ratio of the DVA. The working principle of the DVA did not change since Ormondroyd and Den Hartog's study [2]. However, different designs have been developed that suit different applications. There are many interesting practical applications described by Den Hartog [4] and Hunt [5]. A comprehensive study on the theory and practice of vibration absorbers is given in the book by Korenev and Reznikov [6]. An excellent survey of passive, semiactive, and active DVAs was prepared by Sun et al. [7]. A review of adaptive vibration absorbers, which can adjust their own parameters, can be found in the work of von Flotow et al. [8]. The first researcher that applied the principle of the DVA to a continuous system (i.e., beam) is Young [9]. Snowdon [10] considered the optimization of a discrete absorber on beams with various boundary conditions when structural damping was present. Jacquot [11] has established an analogy between a beam and a SDOF system that allowed the use of the optimal parameters for the latter to determine the corresponding for the beam. Özgüven and Candir [12] have investigated the use of two DVAs to suppress the resonant vibrations associated with the first two natural frequencies. Manikanahally and Crocker [13] extended the work in reference [12] to include point masses in their analysis. Different applications of vibration absorbers can be found in references [14–16].

The problem of a vibrating beam with sprung masses falls in the class of the dynamics of combined systems, which consist of linear elastic structures carrying lumped attachments. The free vibrations of such systems are studied extensively in the literature [17–20]. Literature review indicates that the authors of these papers have generally directed their investigations into finding the natural frequencies and the corresponding mode shapes to evaluate the free vibrations. The most common approach used is the assumed mode method which is one of the approximate methods best suited for solving diverse problems in dynamics and structures (for example, Ginsberg [21]). Other approaches of finding the response of dynamic systems such as finite element, Laplace transform, transfer matrix, and Lagrange multiplier are also used. Cha and Ren [22], utilizing an assumed mode method, used a chain of oscillators to impose nodes (i.e., points of zero displacements) to the normal modes of a beam by properly selecting values for the oscillator parameters (i.e., masses and spring constants) and by properly choosing the attachment location for the oscillator chain. The desired nodes can either coincide with the location of the oscillator chain, or it can be located elsewhere. Using the same method, Cha and Wong [23] analyzed a freely vibrating structure with a series of attached sprung masses aiming to impose multiple nodes for any normal mode. Cha [24] used a set of sprung masses to impose a single or multiple nodes anywhere along a vibrating beam. Alsaif and Foda [25] have applied the dynamic green function to calculate the optimal values of masses and/or springs and their locations along a beam in order to confine the vibration at an arbitrary location. Similarly, Foda and Albassam [26] have exploited Green's function to develop an exact method of analysis for the steady-state response of a harmonically excited Timoshenko beam with attached springs and/or masses and having different boundary conditions with the objective of confining the vibrations along the segment of the beam. Cha and Zhou [27] have created nodes with zero displacements and zero slopes in a harmonically excited linear structure using a set of sprung masses and rotational springs. Cha and Chen [28] have used lumped masses to impose nodes in a harmonically excited flexible beam.

On the contrary, active control methods can be used to create nodal points in continuous systems. Ram [29] has considered the problem of creating a node at the end of an axially vibrating rod using displacement feedback control. He derived a formula for the feedback control gain as a function of the product of the system eigenvalues. This result is based on a relationship derived by Elhay et al. [30] relating the system eigenfunctions to a product of eigenvalues. Singh and Ram [31] have created a node in a vibrating beam using feedback control with a gain calculated from either the infinite product of eigenvalues or deflection data. The implementation of acceleration and displacement feedback control on a beam-type tunable vibration absorber has been considered by Alujevic et al. [32]. They have studied the stability of the feedback loop using the Nyquist criterion.

In the present work, a displacement and velocity feedback active control force is designed for the purpose of enforcing one node, two nodes, and one node with zero slope along any beam during harmonic excitation. The beam is modeled as an Euler–Bernoulli beam that included the effects of internal and external damping. A key feature of this work is that the problem is formulated in terms of dynamic Green's function, which is exact and straightforward. The method is chosen for its freedom from numerical accuracy when compared with the standard application of the modal superposition technique. Furthermore, the boundary conditions are embedded into Green's function of the corresponding beam, and it is not necessary to solve the free vibration problem in order to obtain the eigenvalues and the corresponding eigenfunctions, which are required for modal superposition solution. Equally important, this method exhibits appreciably greater computational efficiency when compared with other methods.

The rest of the paper is organized as follows: Section 2 describes the formulation of the problem and the derivation for the feedback control gain(s) to create one node, two nodes, and one node with zero slope in a harmonically excited beam. Stability analysis and sensor noise rejection

are presented in Sections 3 and 4, while numerical results for the aforementioned cases are displayed in Section 5. Section 6 gives some general conclusions.

2. Problem Formulation

We consider the problem of transverse vibration of a uniform elastic beam of finite length L originally at rest, as shown in Figure 1. The beam can have different classical or unconventional boundary conditions at $x=0$ and $x=L$. The beam is excited by a sinusoidal external force $f_{\text{ext}}(x,t)$ that causes it to vibrate. A control force $u(x,t)$ is designed and applied to the beam in order to reduce or completely eliminate the induced vibrations. The lateral vibration of the beam is governed by the following equations [33]:

$$\begin{aligned}\text{EI}\,\frac{\partial^4 w(x,t)}{\partial x^4}+c_1\frac{\partial w(x,t)}{\partial t}+c_2\frac{\partial^5 w(x,t)}{\partial x^4\partial t}+\rho A\frac{\partial^2 w(x,t)}{\partial t^2}\\ =f_{\text{ext}}(x,t)+u(x,t),\end{aligned}\tag{1}$$

where EI, ρ, A, and $w(x,t)$ denote, respectively, the flexural rigidity of the beam, the density, the cross-sectional area, and the transverse deflection of the beam at point x and time t. The second term represents the external damping effect which is assumed of the viscous type due to friction with the surrounding and has a coefficient c_1. The third term represents the internal damping effect which is assumed to be viscoelastic of the Kelvin-Voigt type with coefficient c_2.

Since damping exists, we will use complex forms for the input force, control force, and the response of the beam. The external excitation force, $f_{\text{ext}}(x,t)$, is assumed to be given by

$$f_{\text{ext}}(x,t)=F_0e^{i\omega t}\delta(x-x_{\text{f}}),\tag{2}$$

where F_0 is the amplitude of the external force, ω is the excitation frequency, $i=\sqrt{-1}$, and x_{f} is the location of the excitation force. The symbol $\delta()$ denotes the Dirac delta function. It is understood that the excitation force is given by the real part of the right-hand side of equation (2).

The control force, $u(x,t)$, which is applied at $x=x_{\text{a}}$ is given by

$$u(x,t)=\left[\alpha_1 w(x_{\text{s}},t)+\alpha_2\frac{\partial w(x_{\text{s}},t)}{\partial t}\right]\delta(x-x_{\text{a}}),\tag{3}$$

where α_1, α_2, and x_{s} are the displacement control gain, velocity control gain, and displacement and velocity sensor location, respectively. At this stage, one can recognize two types of controllers: the collocated type is when the control actuator location (x_{a}) coincides with the sensor location (x_{s}) and the noncollocated type is when the actuator and the sensor have different locations along the beam.

Assuming an applied external force with monochromatic frequency, given by equation (2), the solution of equation (1), using the separation of variables, is sought to have the following form:

$$w(x,t)=W(x)e^{i\omega t},\tag{4}$$

where $W(x)$ is the spatial beam deflection at point x. Substitution of equation (4) into equation (1) reduces it to

$$\begin{aligned}(\text{EI}+i\omega c_2)\frac{d^4W(x)}{dx^4}+\left(i\omega c_1-\rho A\omega^2\right)W(x)\\ =F_0\delta(x-x_{\text{f}})+(\alpha_1+i\omega\alpha_2)W(x_{\text{s}})\delta(x-x_{\text{a}}).\end{aligned}\tag{5}$$

Once again, it is assumed that we are only interested in the real part of the spatial beam deflection $W(x)$.

To make the analysis more general and the problem solution is applicable to a large combinations of system parameters, it is preferred to work with quantities that are nondimensional. Therefore, the following nondimensional variables and coefficients are defined:

$$\begin{aligned}\widehat{x}&=\frac{x}{L},\\ \widehat{W}&=\frac{W}{W_0},\\ \widehat{\omega}&=\frac{\omega}{\omega_0},\end{aligned}\tag{6}$$

where

$$\begin{aligned}W_0&=\frac{F_0L^3}{\text{EI}},\\ \omega_0&=\sqrt{\frac{\text{EI}}{\rho AL^4}},\end{aligned}\tag{7}$$

$$\begin{aligned}\widehat{c}_1&=\frac{\omega_0L^4c_1}{\text{EI}},\\ \widehat{c}_2&=\frac{\omega_0c_2}{\text{EI}},\\ \widehat{\alpha}_1&=\frac{\alpha_1L^3}{\text{EI}},\\ \widehat{\alpha}_2&=\frac{\alpha_2\omega_0L^3}{\text{EI}}.\end{aligned}\tag{8}$$

Substituting the variables and coefficients, in equations (6)–(8), into equation (5) results in the nondimensional form given by

$$\begin{aligned}\widehat{W}''''(\widehat{x})-\frac{\widehat{\omega}^2-i\widehat{\omega}\widehat{c}_1}{1+i\widehat{\omega}\widehat{c}_2}\widehat{W}(\widehat{x})=\frac{1}{1+i\widehat{\omega}\widehat{c}_2}\,\widehat{\delta}(\widehat{x}-\widehat{x}_{\text{f}})\\ +\frac{1}{1+i\widehat{\omega}\widehat{c}_2}\left(\widehat{\alpha}_1+i\widehat{\omega}\widehat{\alpha}_2\right)\\ \cdot\widehat{W}(\widehat{x}_{\text{s}})\widehat{\delta}(\widehat{x}-\widehat{x}_{\text{a}}).\end{aligned}\tag{9}$$

It is to be noted that the prime denotes the derivative with respect to $\widehat{x}$ and $\widehat{\delta}=(1/L)\delta$.

For the sake of convenience, the hat symbol on the dimensionless quantities can be omitted proceeding to find the solution of equation (9) using dynamic Green's function. Denoting $G(x,u)$ as the dynamic Green's function for the stated problem, which is not yet known, the solution of equation (5) can be given by

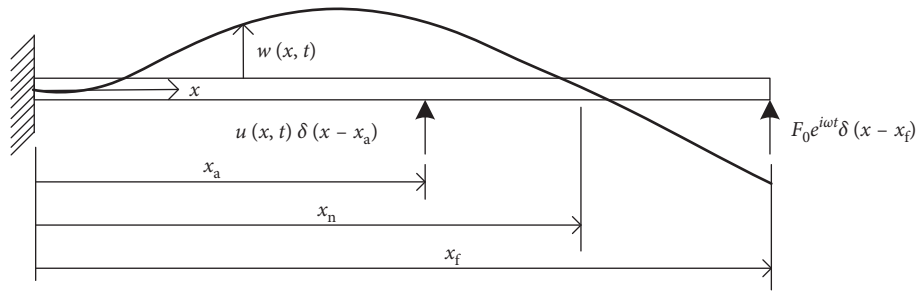

Figure 1: Configuration of a harmonically excited cantilever beam with vibration control force.

$$W(x) = \frac{1}{1 + i\omega c_2}\left[\int_0^L \{G(x,u)\delta(u - x_f) + (\alpha_1 + i\omega\alpha_2) \cdot W(x_s)G(x,u)\delta(u - x_a)\}du\right]. \tag{10}$$

Performing the integration using the properties of the Dirac delta function to obtain

$$W(x) = \frac{1}{1 + i\omega c_2}\left[G(x, x_f) + (\alpha_1 + i\omega\alpha_2)W(x_s)G(x, x_a)\right], \tag{11}$$

where $G(x,u)$ is the solution of the differential equation

$$\frac{d^4G(x,u)}{dx^4} - q^4G(x,u) = \delta(x - u), \tag{12}$$

where the coefficient q^4 is defined by

$$q^4 = \frac{\omega^2 - i\omega c_1}{1 + i\omega c_2}. \tag{13}$$

The solution of equation (12) is reported in references [25, 34] for conventional and nonconventional boundary conditions and will not be repeated here. For example, for a simply supported beam, Green's function takes the following simple form:

$$G(x,u) = \frac{1}{2q^3\sin(qL)\sinh(qL)}\begin{cases} g(x,u), & 0 \le x \le u, \\ g(u,x), & x \le u \le L, \end{cases} \tag{14}$$

where

$$g(x,u) = \sinh(qL)\sin(qx)\sin(qL - qu) - \sin(qL)\sinh(qx)\sinh(qL - qu), \tag{15}$$

and $g(u,x)$ is obtained by replacing x with u in $g(x,u)$.

Dynamic Green's function provides afundamental solution for a differential equation. This function is very useful when dealing with linear systems, for example, books by Roach [35, 36]. Green's function $G(x,u)$ is sometimes called source function, impulse response function, or receptance. It is considered a two-point function of position and is independent of the forcing term. Green's function $G(x,u)$ for a system is defined as the displacement of the system at location x which is due to a unit force applied at location u. It is a symmetric function, in which, $G(x,u)$ is equal to $G(u,x)$, where the latter represents the displacement at point u due to a unit force applied at point x. Therefore, Green's function satisfies the Maxwell–Rayleigh reciprocity law.

To this end, one should note that equation (11) is valid at $x = x_s$ to give

$$W(x_s) = \frac{1}{1 + i\omega c_2}\left[G(x_s, x_f) + (\alpha_1 + i\omega\alpha_2)W(x_s)G(x_s, x_a)\right]. \tag{16}$$

By solving equation (16) for $W(x_s)$, one gets

$$W(x_s) = -\frac{G(x_s, x_f)}{(1 + i\omega c_2) - (\alpha_1 + i\omega\alpha_2)G(x_s, x_a)}. \tag{17}$$

Substituting $W(x_s)$, from equation (17), into equation (11), the steady-state deflection at any point x is, therefore, given by

$$W(x) = \frac{1}{1 + i\omega c_2}\left[G(x, x_f) + \frac{(\alpha_1 + i\omega\alpha_2)G(x_s, x_f)G(x, x_a)}{(1 + i\omega c_2) - (\alpha_1 + i\omega\alpha_2)G(x_s, x_a)}\right]. \tag{18}$$

The expression for $W(x)$, in equation (18), gives the exact closed form solution for the steady-state displacement field of a beam deflection.

2.1. One Node. In this section, it is desired to calculate the control gains that result in creating a node at location x_n on a beam. First, we find the deflection at a specific point x_n along the beam by substituting $x = x_n$ in equation (18) to get

$$W(x_n) = \frac{1}{1 + i\omega c_2}\left[G(x_n, x_f) + \frac{(\alpha_1 + i\omega\alpha_2)G(x_s, x_f)G(x_n, x_a)}{(1 + i\omega c_2) - (\alpha_1 + i\omega\alpha_2)G(x_s, x_a)}\right]. \tag{19}$$

If, in an application, it is required to have a node at a certain location on the beam, for example, $x = x_n$, then one would set $W(x_n)$ equal to zero, to give

$$\frac{1}{1 + i\omega c_2}\left[G(x_n, x_f) + \frac{(\alpha_1 + i\omega\alpha_2)G(x_s, x_f)G(x_n, x_a)}{(1 + i\omega c_2) - (\alpha_1 + i\omega\alpha_2)G(x_s, x_a)}\right] = 0. \tag{20}$$

At this juncture, we utilize the fact that a complex number vanishes if its real and imaginary parts vanish independently. Equation (20) can be arranged and simplified to give

$$\alpha_1 + i\omega\alpha_2 = \frac{(1 + i\omega c_2)G(x_n, x_f)}{G(x_s, x_a)G(x_n, x_f) - G(x_s, x_f)G(x_n, x_a)}. \tag{21}$$

To calculate the gains, α_1 and α_2, we equate the real and imaginary parts of both sides of equation (21), to give

$$\alpha_1 = \mathrm{Re}\left[\frac{(1 + i\omega c_2)G(x_n, x_f)}{G(x_s, x_a)G(x_n, x_f) - G(x_s, x_f)G(x_n, x_a)}\right], \tag{22}$$

$$\alpha_2 = \frac{1}{\omega} \times \mathrm{Im}\left[\frac{(1 + i\omega c_2)G(x_n, x_f)}{G(x_s, x_a)G(x_n, x_f) - G(x_s, x_f)G(x_n, x_a)}\right], \tag{23}$$

where Re[] and Im[] denote the real and imaginary parts of $[\cdot]$, respectively.

Equations (22) and (23) represent the explicit formulas for the control gains which ensure that the vibrational amplitude at $x = x_n$ is equal to zero. This result is better than the one reported by Singh and Ram [31] for an undamped beam because it is exact and does not require infinite product of the eigenvalues of the system.

Equations (22) and (23) represent the general case, in which, the control sensor and actuator are at different locations, i.e., $x_s \neq x_a$, which refers to the noncollocated control case. On the contrary, the control gains for the collocated control case can be calculated by substituting $x_s = x_a$ in equations (22) and (23).

Examining equations (22) and (23), one can observe that if the sensor location coincides with the node location, i.e., $x_s = x_n$, then the denominator of both equations become zero and the control gains approach infinity. This case is expected since the sensor is located at a stationary point where both displacement and velocity are equal to zero. Therefore, it is always required not to place the sensor at the node location. Consequently, if it is desired to create a node at the control actuator location, i.e., $x_n = x_a$, then one should avoid placing the sensor at the actuator location and use the noncollocated control case. In addition, the control gains become infinity if the actuator location coincides with the excitation force location, i.e., $x_a = x_f$. Moreover, if the system is undamped ($c_1 = c_2 = 0$), then Green's function becomes a real valued function where α_2, from equation (23), is equal to zero, which means that a node cannot be imposed by a control force that is proportional to both beam displacement and velocity at the sensor position. Instead, a node can be enforced at any location by using a control force that is proportional to the beam displacement only. A comparable situation is encountered in the theory of vibration absorber, where one cannot introduce antiresonance in a system consisting of an undamped primary system and a damped DVA as an auxiliary attachment.

It is to be noted that if the sensor location coincides with the actuator location and the control gains are negative, then the control action can be implemented using passive elements. In other words, the control can be realized by a spring of stiffness equals $-\alpha_1$ and a damper with damping constant equals $-\alpha_2$, both are connected in parallel between the ground and the beam at the actuator location (x_a).

2.2. Two Nodes. In this section, we demonstrate a numerical method to impose two nodes in a vibrating beam subjected to a harmonic force by applying two control forces at specific locations on the beam using Green's function. Our goal here is to determine the values of the control forces required. The net control force $u(x,t)$ formed by the summation of the two control forces applied at locations x_{a_1} and x_{a_2} is given by

$$u(x,t) = \left[\alpha_1 w(x_{s_1}, t) + \alpha_2 \frac{\partial w(x_{s_1}, t)}{\partial t}\right]\delta(x - x_{a_1}) + \left[\alpha_3 w(x_{s_2}, t) + \alpha_4 \frac{\partial w(x_{s_2}, t)}{\partial t}\right]\delta(x - x_{a_2}), \tag{24}$$

where x_{s_1} and x_{s_2} are the locations of the sensors for measuring the displacement and velocity amplitudes for the two control forces, respectively. Similar to the one node case, the nondimensional governing equation of the system takes the following form:

$$\begin{aligned}\widehat{W}''''(\widehat{x}) - \frac{\widehat{\omega}^2 - i\widehat{\omega}\widehat{c}_1}{1 + i\widehat{\omega}\widehat{c}_2}\widehat{W}(\widehat{x}) = {} & \frac{1}{1 + i\widehat{\omega}\widehat{c}_2}\widehat{\delta}(\widehat{x} - \widehat{x}_f) \\ & + \frac{1}{1 + i\widehat{\omega}\widehat{c}_2}[(\widehat{\alpha}_1 + i\widehat{\omega}\widehat{\alpha}_2)\widehat{W}(\widehat{x}_{s_1}) \\ & \cdot \widehat{\delta}(\widehat{x} - \widehat{x}_{a_1}) + (\widehat{\alpha}_3 + i\widehat{\omega}\widehat{\alpha}_4) \\ & \cdot \widehat{W}(\widehat{x}_{s_2})\widehat{\delta}(\widehat{x} - \widehat{x}_{a_2})].\end{aligned} \tag{25}$$

Similar to equation (11), the solution of the aforementioned equation takes the form

$$\begin{aligned}\widehat{W}(\widehat{x}) = \frac{1}{1 + i\omega\widehat{c}_2}\Big[& G(\widehat{x}, \widehat{x}_f) + (\widehat{\alpha}_1 + i\omega\widehat{\alpha}_2)\widehat{W}(\widehat{x}_{s_1})G(\widehat{x}, \widehat{x}_{a_1}) \\ & + (\widehat{\alpha}_3 + i\omega\widehat{\alpha}_4)\widehat{W}(\widehat{x}_{s_2})G(\widehat{x}, \widehat{x}_{a_2})\Big].\end{aligned} \tag{26}$$

For notational simplicity and convenience, we drop the hat symbol in equation (26) and follow the same steps as in the one node case to calculate the control gains α_1, α_2, α_3, and α_4, which are as follows:

(1) Substitute $x = x_{s_1}$ and $x = x_{s_2}$ in equation (26) to form two equations

(2) Solve for $W(x_{s_1})$ and $W(x_{s_2})$ from the two equations in Step 1 and substitute them back into $W(x)$ in equation (26)

(3) Substitute $x = x_{n_1}$ and $x = x_{n_2}$ in the equation of $W(x)$ formed in Step 2 to form the following two equations to solve for the control gains α_1, α_2, α_3, and α_4

$$W\left(x_{n_1}\right) = 0, \tag{27a}$$

$$W\left(x_{n_2}\right) = 0. \tag{27b}$$

It is to be noted that equations (27a) and (27b) generate the two desired nodes on the beam.

After applying the above steps, one can obtain the following results:

$$W\left(x_{s_1}\right) = -\frac{AG_{s_1 f} + CG_{s_1 a_2}G_{s_2 f} - CG_{s_1 f}G_{s_2 a_2}}{ABG_{s_1 a_1} - A^2 + ACG_{s_2 a_2} - BCG_{s_1 a_1}G_{s_2 a_2} + BCG_{s_1 a_2}G_{s_2 a_1}}, \tag{28a}$$

$$W\left(x_{s_2}\right) = -\frac{AG_{s_2 f} - BG_{s_1 a_1}G_{s_2 f} + BG_{s_1 f}G_{s_2 a_1}}{ABG_{s_1 a_1} - A^2 + ACG_{s_2 a_2} - BCG_{s_1 a_1}G_{s_2 a_2} + BCG_{s_1 a_2}G_{s_2 a_1}}, \tag{28b}$$

where $W(x_{s_1})$ and $W(x_{s_2})$ are the steady-state amplitude of the beam at the sensor locations x_{s_1} and x_{s_2}, respectively, and A, B, and C are given by

$$\begin{aligned} A &= 1 + i\omega c_2, \\ B &= \alpha_1 + i\omega\alpha_2, \\ C &= \alpha_3 + i\omega\alpha_4, \end{aligned} \tag{29}$$

and $G_{ij} = G(x_i, x_j)$.

Solving equations (27a) and (27b) for B and C to get

$$B = \frac{A\left(G_{n_2 f}G_{n_1 a_2} - G_{n_1 f}G_{n_2 a_2}\right)}{G_{s_1 a_1}G_{n_2 f}G_{n_1 a_2} - G_{s_1 a_2}G_{n_2 f}G_{n_1 a_1} - G_{s_1 a_1}G_{n_1 f}G_{n_2 a_2} + G_{s_1 a_2}G_{n_1 f}G_{n_2 a_1} + G_{s_1 f}G_{n_1 a_1}G_{n_2 a_2} - G_{s_1 f}G_{n_1 a_2}G_{n_2 a_1}}, \tag{30a}$$

$$C = -\frac{A\left(G_{n_2 f}G_{n_1 a_1} - G_{n_1 f}G_{n_2 a_1}\right)}{G_{s_2 a_1}G_{n_2 f}G_{n_1 a_2} - G_{s_2 a_2}G_{n_2 f}G_{n_1 a_1} - G_{s_2 a_1}G_{n_1 f}G_{n_2 a_2} + G_{s_2 a_2}G_{n_1 f}G_{n_2 a_1} + G_{s_2 f}G_{n_1 a_1}G_{n_2 a_2} - G_{s_2 f}G_{n_1 a_2}G_{n_2 a_1}}. \tag{30b}$$

From equations (29) for B and C, the control gains are given by

$$\begin{aligned} \alpha_1 &= \mathrm{Re}[B], \\ \alpha_2 &= \frac{1}{\omega}\mathrm{Im}[B], \end{aligned} \tag{31a}$$

$$\begin{aligned} \alpha_3 &= \mathrm{Re}[C], \\ \alpha_4 &= \frac{1}{\omega}\mathrm{Im}[C]. \end{aligned} \tag{31b}$$

It is to be noted that this case represents a noncollocated case, in which the locations of the control sensors are different from the locations of the control actuators. The control force gains for the collocated case can be easily obtained by substituting $x_{s_1} = x_{a_1}$ and $x_{s_2} = x_{a_2}$ in equations (30a) and (30b).

2.3. One Node with Zero Slope. In this section, we demonstrate a numerical method to impose one node with zero displacements and zero slopes in a vibrating beam subjected to a harmonic force by applying two control forces at specific locations on the beam using Green's function. The advantage of having the slope of the displacement at the node to be zero is the improved robustness by increasing the interval of zero displacements near the node. Our goal here is to determine the values of the control forces required. The equations involving $u(x,t)$, the equation of motion, and its solution are given in equations (24)–(26) given in Section 2.2.

The following steps are applied in order to calculate the control gains α_1, α_2, α_3, and α_4:

(1) Substitute $x = x_{s_1}$ and $x = x_{s_2}$ in equation (26) to form two equations

(2) Solve for $W(x_{s_1})$ and $W(x_{s_2})$ from the two equations in Step 1 and substitute them back into $W(x)$ in equation (26)

(3) Substitute $x = x_n$ in the equation of $W(x)$ formed in Step 2

(4) Solve for the control gains α_1, α_2, α_3, and α_4 from the following two equations:

$$W(x_n) = 0, \tag{32a}$$

$$\frac{dW(x_n)}{dx} = 0. \tag{32b}$$

Equations (32a) and (32b) are responsible for generating a node at a desired location (x_n) on the beam having both zero displacements and zero slopes.

After applying the above steps, one can obtain the equations for $W(x_{s_1})$ and $W(x_{s_2})$ which are the same as that given by equations (28a) and (28b). The solutions for B and C are given by

$$B = \frac{A\left(G_{na_2}G'_{nf} - G'_{na_2}G_{nf}\right)}{G_{s_1a_1}G_{na_2}G'_{nf} - G_{s_1a_1}G'_{na_2}G_{nf} - G_{s_1a_2}G_{na_1}G'_{nf} + G_{s_1a_2}G'_{na_1}G_{nf} + G_{s_1f}G_{na_1}G'_{na_2} - G_{s_1f}G_{na_2}G'_{na_1}}, \tag{33a}$$

$$C = \frac{A\left(G'_{na_1}G_{nf} - G_{na_1}G'_{nf}\right)}{G_{s_2a_1}G_{na_2}G'_{nf} - G_{s_2a_1}G'_{na_2}G_{nf} - G_{s_2a_2}G_{na_1}G'_{nf} + G_{s_2a_2}G'_{na_1}G_{nf} + G_{s_2f}G_{na_1}G'_{na_2} - G_{s_2f}G_{na_2}G'_{na_1}}, \tag{33b}$$

where $()'$ denotes differentiation with respect to x. The control gains, $\alpha_1, \alpha_2, \alpha_3$, and α_4, can be calculated using equations (31a), (31b), and (29).

This case represents the noncollocated case, in which the control sensors are located in different locations from the control actuators. On the contrary, the gains for the collocated control case can be calculated by substituting $x_{s_1} = x_{a_1}$ and $x_{s_2} = x_{a_2}$ in equations (33a) and (33b).

3. Stability Analysis

It has been shown that the control gains to impose a node in a beam structure can be either positive or negative. If they are negative, then the control can be implemented by using passive elements. This is done by attaching to the ground a spring of constant $k = -\alpha_1$ and a damper with damping constant $c = -\alpha_2$ at the control force actuator location.

If the system is undamped, then it has been shown that a node can be imposed by using only displacement feedback with a control gain α. In this case, Singh and Ram [31] have shown that the controlled system is stable if and only if

$$\alpha < \frac{1}{d}, \tag{34}$$

where d is the static deflection of the beam due to a unit control force applied at the control actuator location (x_a). Since d is always positive, the inequality (34) holds whenever the value of the control gain α is negative. In this case, it is concluded that the controlled system is stable. When the beam structure is damped, imposing a node requires velocity feedback signal with gain α_2 in addition to the displacement feedback signal with gain α_1. It is assumed that α_1 satisfies the stability condition (34). If the value of α_2 is negative, then this is equivalent to attaching a damper with damping coefficient $c = -\alpha_2$ at the location of the control actuator (x_a). Since the damping coefficient c is positive, the damper will dissipate beam energy, and, therefore, the controlled beam is stable. On the contrary, if the velocity feedback control gain α_2 is positive, then the stability can be examined by discretizing the equation of motion, equation (1), after substituting equations (2) and (3).

Using the assumed modes method, the transverse deflection of the beam $w(x,t)$ can be approximated using

$$w(x,t) = \sum_{i=1}^{n} \phi_i(x)\eta_i(t), \tag{35}$$

where $\phi_i(x)$ denotes the i^{th} assumed mode shape, $\eta_i(t)$ denotes the i^{th} generalized coordinate, and n denotes the number of terms retained in the approximation. The kinetic energy of the beam structure can be written as

$$T = \frac{1}{2}\int_0^L \rho A\left(\frac{\partial w(x,t)}{\partial t}\right)^2 dx, \tag{36}$$

and the potential energy is given by

$$U = \frac{1}{2}\int_0^L \text{EI}\left(\frac{\partial^2 w(x,t)}{\partial x^2}\right)^2 dx. \tag{37}$$

The virtual work done by the external forces (nonconservative forces) can be expressed as

$$W_{nc} = \int_0^L p(x,t)w(x,t)\,dx, \tag{38}$$

where $p(x,t)$ represents the external applied force per unit length of the beam as well as the damping effects and the control terms and is given by

$$p(x,t) = \text{Re}\left[F_0 e^{i\omega t}\right]\delta(x - x_f) - c_1\frac{\partial w(x,t)}{\partial t} - c_2\frac{\partial^5 w(x,t)}{\partial t \partial x^4} + \left[\alpha_1 w(x_s,t) + \alpha_2\frac{\partial w(x_s,t)}{\partial t}\right]\delta(x - x_a), \tag{39}$$

where all the terms are defined in the previous sections.

By substituting equation (35) into equations (36)–(38) and performing all the integrations and applying Lagrange's equations,

$$\frac{d}{dt}\left(\frac{\partial T}{\partial \dot{\eta}_i}\right) - \frac{\partial T}{\partial \eta_i} + \frac{\partial U}{\partial \eta_i} = Q_i, \quad i = 1, 2, \ldots, n. \tag{40}$$

The following discretized equations of motion, in the matrix form, can be derived:

$$M\ddot{\boldsymbol{\eta}} + (C - C_a)\dot{\boldsymbol{\eta}} + (K - K_a)\boldsymbol{\eta} = \mathbf{Q}, \tag{41}$$

where

$$
\begin{aligned}
M &= \rho A \int_0^L \boldsymbol{\phi}\boldsymbol{\phi}^T \, dx, \\
C &= c_1 \int_0^L \boldsymbol{\phi}\boldsymbol{\phi}^T \, dx + c_2 \int_0^L \boldsymbol{\phi}''''\boldsymbol{\phi}^T \, dx, \\
K &= \mathrm{EI} \int_0^L \boldsymbol{\phi}''\boldsymbol{\phi}''^T \, dx, \\
K_a &= \alpha_1 \boldsymbol{\phi}(x_s)\boldsymbol{\phi}^T(x_a), \\
C_a &= \alpha_2 \boldsymbol{\phi}(x_s)\boldsymbol{\phi}^T(x_a), \\
\mathbf{Q} &= \mathrm{Re}\left[F_0 e^{i\omega t}\right]\boldsymbol{\phi}(x_f),
\end{aligned}
\tag{42}
$$

where M, C, K, C_a, and K_a are $n \times n$ matrices, $\mathbf{Q}$ is an $n \times 1$ vector, $()'$ denotes the differentiation with respect to x, $()^T$ denotes the transpose, and the $n \times 1$ vectors $\boldsymbol{\phi}$ and $\boldsymbol{\eta}$ are defined by

$$
\begin{aligned}
\boldsymbol{\phi}(x) &= \left[\phi_1(x)\ \phi_2(x) \cdots\ \phi_n(x)\right]^T, \\
\boldsymbol{\eta}(t) &= \left[\eta_1(t)\ \eta_2(t)\ \cdots\ \eta_n(t)\right]^T.
\end{aligned}
\tag{43}
$$

Equation (41) can be transformed to a state-space form by defining the following states:

$$
\mathbf{z}_1 = \boldsymbol{\eta}, \tag{44a}
$$

$$
\mathbf{z}_2 = \dot{\boldsymbol{\eta}}, \tag{44b}
$$

to give the state equation

$$
\dot{\mathbf{z}} = \mathbf{A}\mathbf{z} + \mathbf{B}u^*, \tag{45}
$$

where $\mathbf{z}$ is the $2n \times 1$ state vector, $\mathbf{A}$ is the $2n \times 2n$ system matrix, $\mathbf{B}$ is the $2n \times 1$ input vector, and u^* is a scalar input, which are given by

$$
\begin{aligned}
\mathbf{A} &= \begin{bmatrix} 0_{n\times n} & I_{n\times n} \\ -M^{-1}(K - K_a) & -M^{-1}(C - C_a) \end{bmatrix}, \\
\mathbf{B} &= \begin{bmatrix} \mathbf{0}_{n\times 1} \\ M^{-1}\boldsymbol{\phi}(x_f) \end{bmatrix}, \\
u^* &= \mathrm{Re}\left[F_0 e^{i\omega t}\right].
\end{aligned}
\tag{46}
$$

The following comparison function $\phi_i(x)$ is chosen as the assumed modes shape:

$$
\phi_i(x) = 1 - \cos\left(\frac{i\pi x}{L}\right) + \frac{1}{2}(-1)^{i+1}\left(\frac{i\pi x}{L}\right)^2, \tag{47}
$$

which satisfies both the geometric and natural boundary conditions of a cantilever beam.

The stability of the controlled beam structure can be evaluated by calculating the eigenvalues of the system matrix $\mathbf{A}$. For a stable system, all the eigenvalues of the system matrix must have a negative real part and marginally stable if any of the eigenvalues have zero real parts.

4. Sensor Noise Rejection

In this section, the effect of sensor noise on the system response is analyzed by using the state-space model in equation (46). The states represent the generalized modal coordinates which are related to the beam deflection ($w(x,t)$) through equation (35). Since a sensor noise affects the measurements of the beam deflection, mathematically it will affect the values of the generalized modal coordinates. Consequently, to study the effect of sensor noise on the response and then try to eliminate its effect, a noisy input is added to the sinusoidal input of the state-space model to generate a noisy signal at the output.

The state-space model for a controlled cantilever beam is given by the state equations, equation (45), along with the output equation given by

$$
\mathbf{y} = \mathbf{C}^*\mathbf{z} + \mathbf{D}u^*, \tag{48}
$$

where $\mathbf{y}$ is an $r \times 1$ output vector, $\mathbf{C}^*$ is an $r \times 2n$ output matrix, and $\mathbf{D}$ is an $r \times 1$ feedforward matrix.

To obtain the deflection of the beam at any location, the system represented by equations (45) and (48) is solved for the state-space vector ($\mathbf{z}(t)$) due to a sinusoidal input. If the desired output of the state-space model is the deflection of the beam at the sensor location ($w(x_s,t)$), then the $1 \times 2n$ output matrix ($\mathbf{C}^*$) and the 1×1 feedforward matrix ($\mathbf{D}$) are given by

$$
\begin{aligned}
\mathbf{C}^* &= \left[\ \boldsymbol{\phi}(x_s)^T\ \ \mathbf{0}_{1\times n}\ \right], \\
\mathbf{D} &= 0.
\end{aligned}
\tag{49}
$$

To verify the accuracy of the state-space model, the beam deflection at the sensor location calculated using the state-space model is compared with that obtained from Green's function method.

A simple low-pass filter design is performed using Simulink. A Simulink block diagram is created that is comprised of a noisy input signal, the state-space model, a low-pass filter, and an output port. The input to the system is a sinusoidal input with an added random signal with Gaussian distribution. The low-pass filter is given by the first-order transfer function:

$$
G_F(s) = \frac{a}{s + a}, \tag{50}
$$

where a is a constant selected based on the parameters of the input and the beam system and s represents the complex Laplace variable. This filter has a cutoff frequency of a rad/s.

5. Simulations and Discussion

In this section, different numerical experiments are carried out to demonstrate the applicability of the proposed approach for creating single node, two nodes, and a single node with zero slopes during harmonic excitations of beams. Cases where active and passive means for vibration control, in addition to collocated and noncollocated control cases, are investigated, and system stability analysis is performed. Furthermore, the numerical technique is applied to beams with different end supports. The last section demonstrates a simple filter design using Simulink to eliminate the noisy signal produced by the sensor that can affect the performance of the controller.

Nondimensional quantities, defined in equations (6)–(8), are used in the numerical examples which can be

transformed to their dimensional counterpart once all the parameters of the beam structure are defined.

5.1. One Node. Consider a uniform cantilever beam of length $L = 1$, excited by a concentrated harmonic force of amplitude $F_0 = 1$, an excitation frequency $\omega = 30$, and excitation location $x_f = 1$. The external damping coefficient $c_1 = 0.1$, while the internal damping coefficient $c_2 = 0.001$. For a given application, a node is desired at the location of the force, i.e., $x_n = x_f$. The steady-state lateral deflection of the beam is shown in Figure 2. The solid curve corresponds to the deformed shape of the beam with a control force acting at position $x_a = 0.55$, which coincides with the location of the control sensor (x_s) (i.e., collocated). The dashed curve corresponds to the deformed shape of the beam with no control force, and the zero horizontal line represents the configuration of the undeformed beam. The control gains are $\alpha_1 = -317.159$ and $\alpha_2 = 0.201$, and the corresponding amplitude of the control force is $|u| = 2.710$. As seen in Figure 2, the point $x_n = x_f$ remains stationary if the control force with the proper chosen gains is applied. The casual observer may doubt the results shown in Figure 2 arguing that since a node exists at the location of the excitation force, the deflection along the whole beam span should be zero because the work of the excitation force is zero. A similar situation occurs in the undamped DVA theory that can remove this suspicion. The excitation force that acts on the primary mass results in the vibration of both masses, namely, the primary mass and the absorber mass. However, when the tuning is satisfied, the primary mass becomes motionless, with no work being injected into the system, but the absorber mass keeps vibrating. The book by Ginsberg [21] has a good discussion on this subject.

The stability of the beam system in this example can be examined using the analysis in Section 3. The system matrix and the input vector, in equation (45), are computed using the dimensional parameters of the beam structure, $EI = 5\,N{\cdot}m^2$, $\rho A = 3\,kg/m$, $L = 1\,m$, and $F_0 = 1\,N$. The number of generalized coordinates used in the simulation is 100. The eigenvalues of the system matrix are computed using Matlab. All the calculated eigenvalues have negative real parts proving the controlled beam to be stable. The time simulation for all the generalized coordinates ($\eta_i(t)$) due to a unit impulse input applied at the excitation force location (x_f) is shown in Figure 3.

Figure 4 shows the design plots of the required control gains and the amplitude of the control force versus the location of the control actuator (x_a) for the same frequency, damping, excitation force location, and node location associated with Figure 2. Considerable information related to stability, optimality, and type of control can be drawn from this figure. Here the optimality is based on the minimum control force requirement. The control gains near $x_a = 0$ are very large because the displacement amplitude $W(x_a)$ is almost equal to zero. Moreover, the control force at $x_a = 0$ is equal to zero since the displacement amplitude at the fixed end is equal to zero. On the contrary, the control gains which are needed to achieve no steady-state motion at the free end are infinite because the displacement is required to be zero, but the control force amplitude has to be equal to -1. Furthermore, it is noted that the feedback control gain, α_1, experiences local maximum and minimum, whereas the feedback control gains, α_2, experience a local maximum at the two control force locations, $x_a = 0.34$ and $x_a = 0.82$. This is due to the coincidence of the control force location with a node created in the controlled beam deflection.

It is to be noted that the control gains α_1 and α_2 can have positive or negative values depending on the system and the control parameters. Consequently, the control force for which the control gains are negative can be implemented by using passive elements, i.e., springs and dampers.

The issue of robustness is more critical than the issue of optimality of the control force. This is clearly obvious because at the free end, the control force requirement is a minimum but the control gain is infinity. The range for the control gains, along the beam, having a flat shape is a sign of robustness.

Figure 5 shows the required control gains and the amplitude of the control force in terms of the excitation frequency for the same system parameters given in Figure 2. It is noted that the control gains, α_1, experience local maximum and minimum, whereas the control gains, α_2, experience a local maximum at the two excitation force frequencies, $\omega = 32.83$ and $\omega = 144$. This is due to the coincidence of the control force location with a node created in the controlled beam deflection at these two frequencies. Furthermore, the amplitude of the control force is almost zero when the excitation force frequency is $\omega = 15.42$ because the controlled and uncontrolled beam deflection coincide with each other at this frequency and a node is created at the free end without the need for a control force. Similar behavior occurs at the excitation force frequency $\omega = 50$. In conclusion, and for a given excitation force frequency, node location, and damping coefficients, one should place the control force actuator that results in minimizing the control force magnitude.

The steady-state deformed shape of a uniform undamped cantilever beam subjected to a localized harmonic force applied at $x_f = 0.5$ with a forcing frequency $\omega = 61.68$, which is near the beam third nondimensional natural frequency, is shown in Figure 6. It is desired to have a node at $x_n = 0.8$ with a control actuator located at $x_a = 0.3$. The control gains are $\alpha_1 = 20.347$ and $\alpha_2 = 0$, and the corresponding amplitude of the control force $|u| = 0.0267$. The beam with control force has a node at exactly $x_n = 0.8$, and it experiences substantially less vibration compared to the uncontrolled beam. Since the value of the control gain is positive, the stability of the controlled beam needs to be examined using condition (34). The control gain (α_1) and the inverse of the beam static deflection due to a unit control force applied at the control actuator location (x_a) versus the control actuator location (x_a) is shown in Figure 7 and its zoomed counterpart in Figure 8. It is apparent from Figure 7 that the actively controlled system is stable when the position of control force is between $0 \ll x_a \ll 0.47$, $0.50 \ll x_a \ll 0.72$ and $0.80 \ll x_a \ll 0.94$. Furthermore, it is clear from Figure 8 that the value of the control gain (α_1), at the control actuator

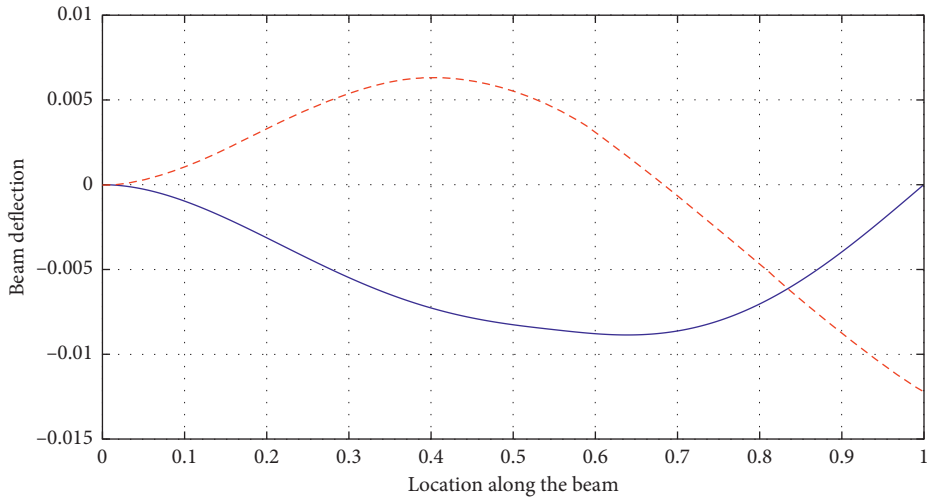

Figure 2: The steady state deformed shape of a collocated controlled (solid line) and uncontrolled (dashed line) damped cantilever beam when $c_1 = 0.1$, $c_2 = 0.001$, $\omega = 30$, $x_f = 1$, $x_n = 1$, and $x_a = 0.55$.

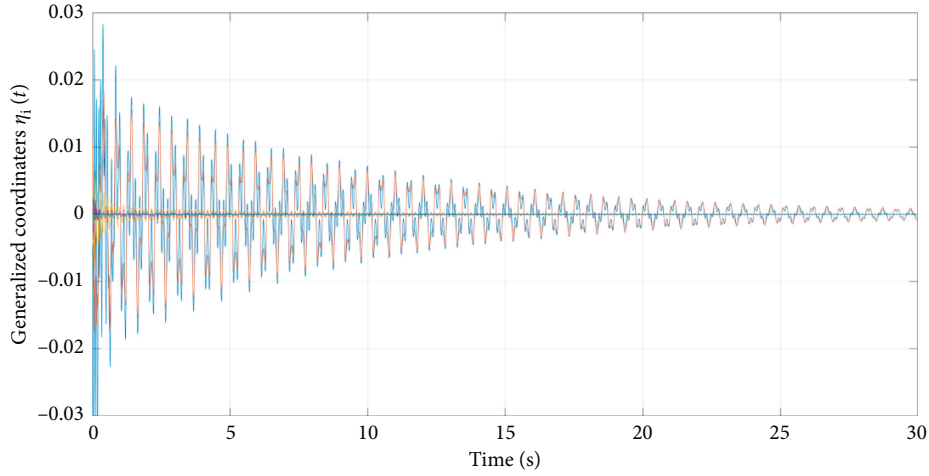

Figure 3: Generalized coordinates $\eta_i(t)$ for the beam system in Figure 2 due to a unit impulse input.

location ($x_a = 0.3$), is less than the value of the inverse of the static deflection ($1/d$), and therefore, the controlled beam system is stable.

In certain applications, it is desired to place the actuator at the required node location, i.e., $x_a = x_n$. In this case, it is compulsory to place the sensor at a location x_s that does not coincide with x_a. This situation is shown in Figure 9, in which a node is desired to be created at the control actuator location, namely, $x_n = x_a = 0.4$, in an undamped simply supported beam. The sensor position is at $x_s = 0.75$ and the excitation force frequency $\omega = 42$. The required control gains are $\alpha_1 = -269.566$ and $\alpha_2 = 0$, and the corresponding amplitude of the control force is $|u| = 0.8533$.

Figure 10 displays the steady-state deformed shape of an undamped simply supported beam subjected to a concentrated harmonic excitation force with a frequency $\omega = 246.73$ which nearly coincides with nondimensional fifth natural frequency of the uncontrolled beam given by $25\pi^2$. The external force acts at $x_f = 0.77$, and the node is required to be imposed at the excitation force location, i.e., $x_n = 0.77$. A control force which is proportional to the displacement is applied at $x_a = 0.9$ to achieve the aforementioned requirement. The required control gains are $\alpha_1 = -1507.459$ and $\alpha_2 = 0$, and the corresponding amplitude of the control force is $|u| = 0.45355$. This figure indicates that the controlled beam is practically motionless. The underlying reason for this behavior is that if the system is driven at resonant frequency, only one mode that represents a flexural wave contributes to the beam deformation. Therefore, if the control force is applied, it creates an antiwave so that when it is added to the original flexural wave, the result is no vibration.

In comparison with other numerical methods to impose a node with zero displacements, Example (1) of Singh and Ram [31] is considered. They considered an undamped Euler–Bernoulli cantilever beam of length $L = 2$, $EI = 5$, $\rho A = 3$, $F_0 = 2$, $\omega = 10$, and $x_f = 2$ all with appropriate units. The control force location $x_a = 0.75$. Their objective is to determine the feedback control force gain needed to eliminate the motion at the free end, i.e., $x_n = 2$. The

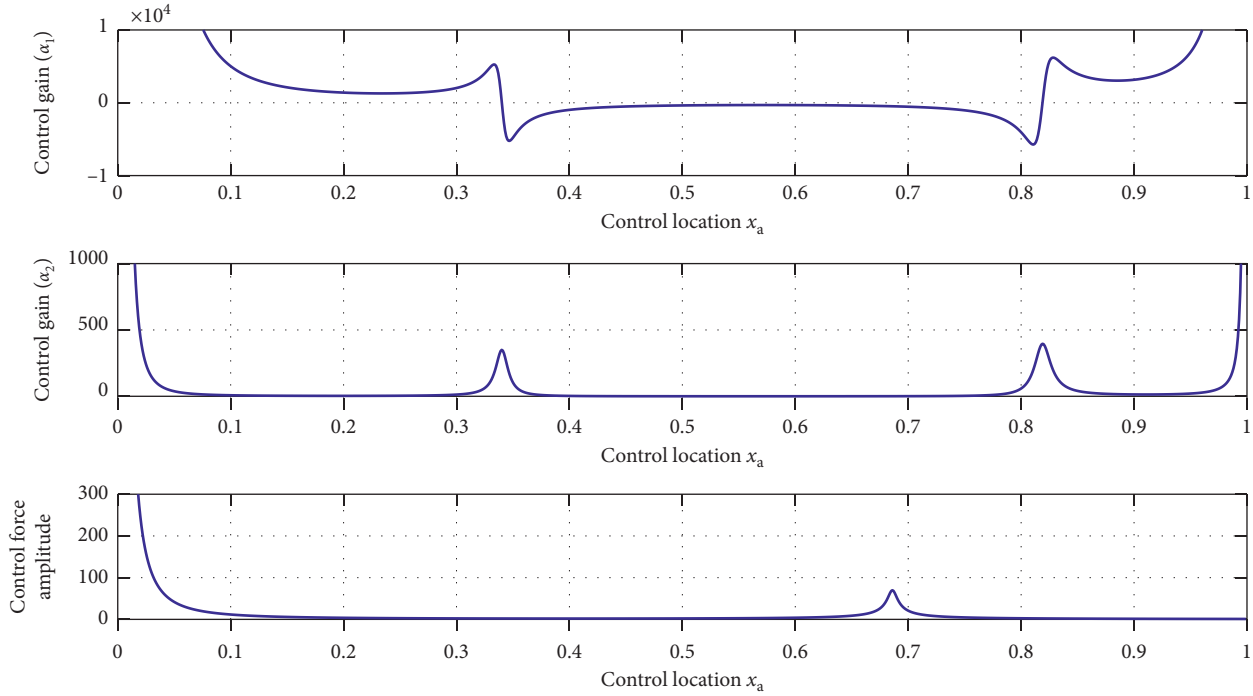

FIGURE 4: The design plot of the required control gains and amplitude versus control actuator location.

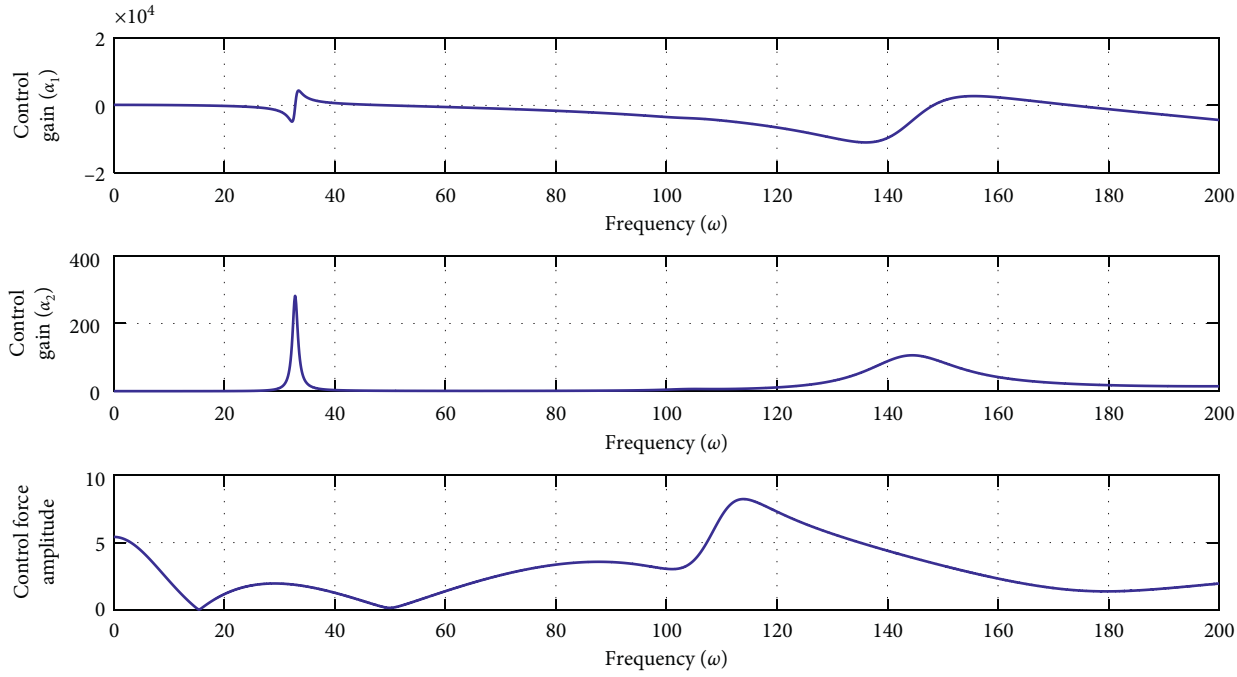

FIGURE 5: The design plot of the required gains versus the excitation frequency ω/ω_0 for the same x_f, x_n of the cantilever beam of Figure 2.

measurement location (x_s) is at 0.75 (collocated case). They used a numerical method based on deformation that divides the beam into two parts and solves two differential equations for the beam deflection amplitudes to obtain the control gain (α). Their other method of solution is to express the control gain in terms of an infinite product of eigenvalues. The calculated control gain is $\alpha = -1781.5$.

Using Green's function, the above parameters are transformed into a nondimensional form using equations (6) and (7) as $\widehat{x}_n = 1$, $\widehat{x}_a = 0.375$, $\widehat{x}_f = 1$, $\widehat{x}_s = 0.375$, and $\widehat{\omega} = 10/\sqrt{(5/48)} = 30.984$. The numerical procedure in Section 2.1 is used to calculate the control gain ($\widehat{\alpha}$) to obtain a value of −2850.4259949 (nondimensional). The dimensional control gain (α) can be calculated using equation (8),

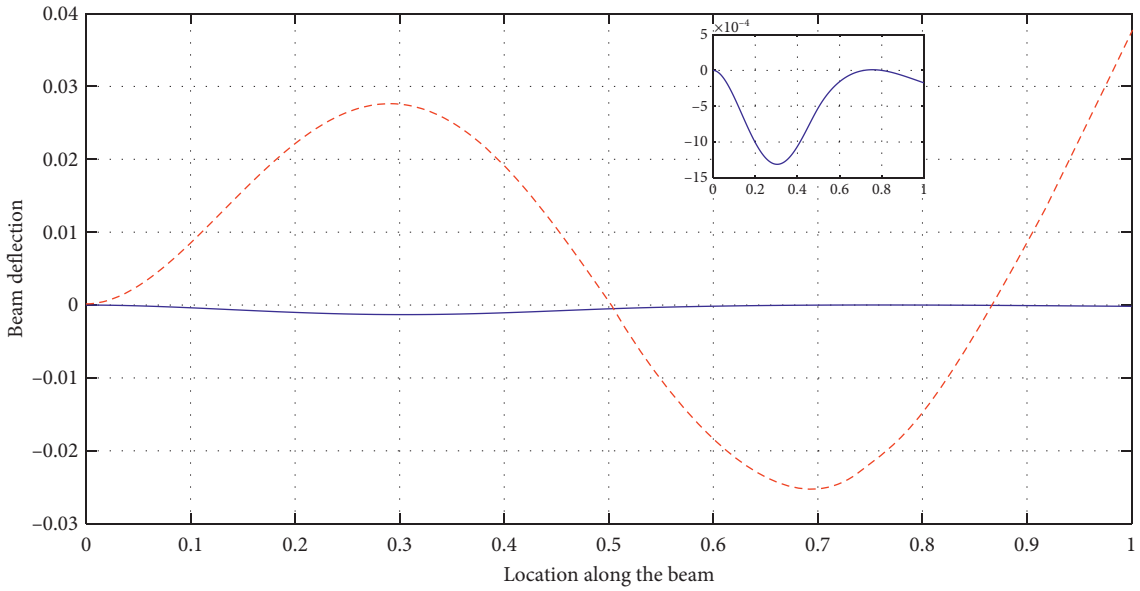

Figure 6: The steady-state deformed shape of a collocated controlled (solid line) and uncontrolled (dashed line) undamped cantilever beam when $\omega = 61.68$, $x_f = 0.5$, $x_n = 0.8$, and $x_a = 0.3$. The small figure shows a detailed plot of the controlled shape.

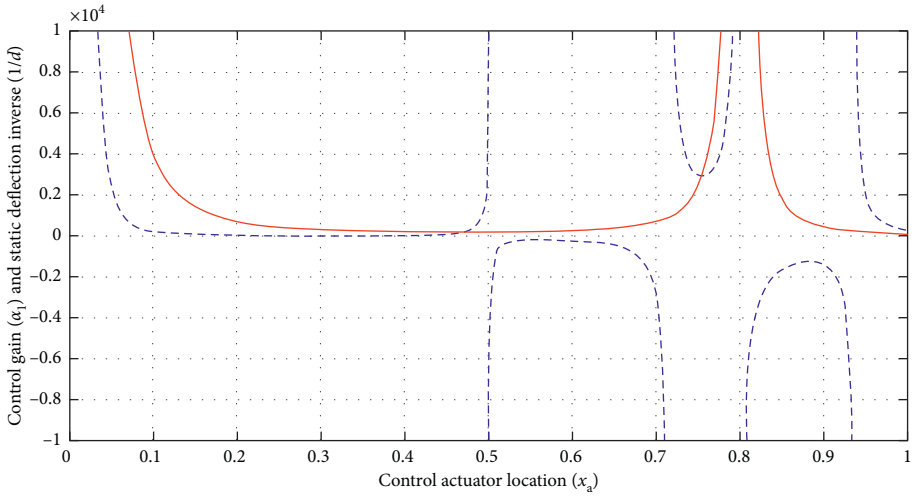

Figure 7: Control gain (α_1), - - -, and inverse of the static deflection ($1/d$), ——, for $0 \le x_a \le 1$.

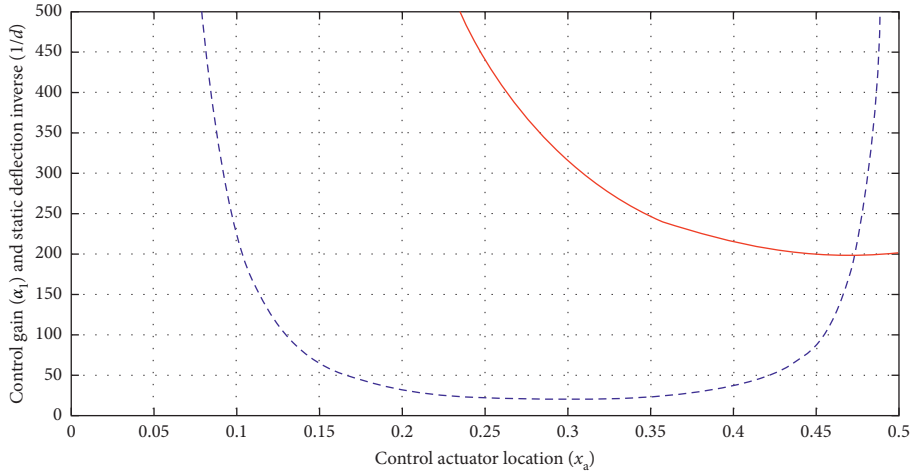

Figure 8: Zoomed control gain (α_1), - - -, and inverse of the static deflection ($1/d$), ——, for $0 \le x_a \le 0.5$.

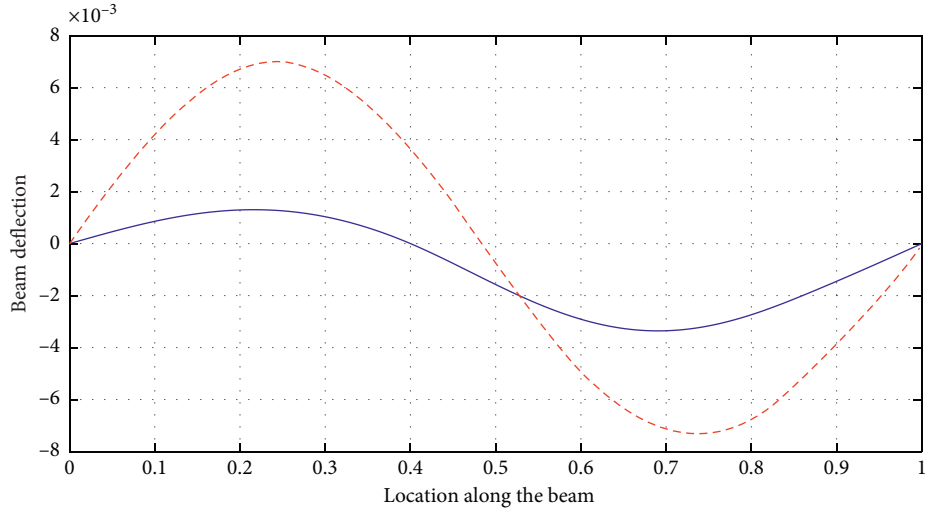

Figure 9: The steady-state deformed shape of a noncollocated controlled (solid line) and uncontrolled (dashed line) undamped simply supported beam when $\omega = 42$, $x_f = 0.87$, $x_n = 0.4$, $x_a = 0.4$, and $x_s = 0.75$.

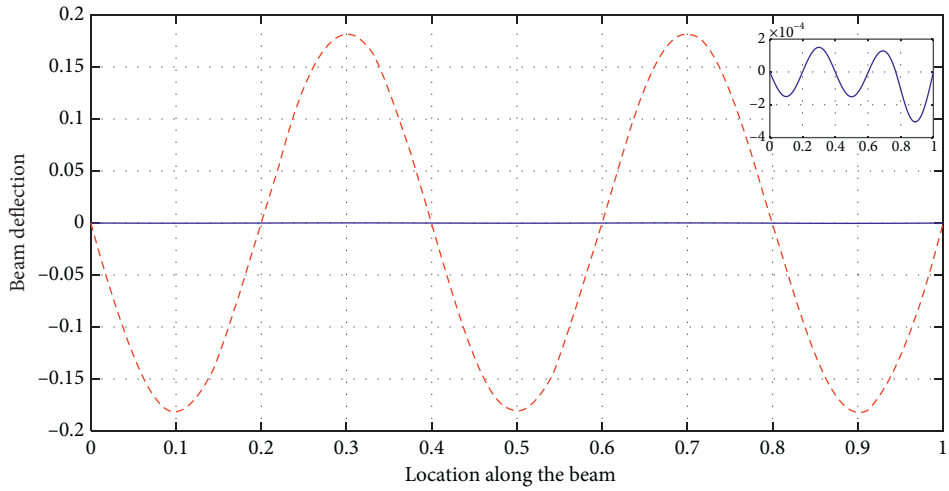

Figure 10: The steady-state deformed shape of a collocated controlled (solid line) and uncontrolled (dashed line) undamped simply supported beam when $\omega = 246.73$, $x_f = 0.77$, $x_n = 0.77$, and $x_a = 0.9$. The inset shows the detailed plot of the controlled shape.

$\alpha = (\hat{\alpha}EI)/L^3 = (-2850.4259949 \times 5)/2^3 = -1781.5162468$, which is exactly the same value as that obtained by Singh and Ram. A plot of the steady-state beam deflection is shown Figure 11.

5.2. Two Nodes. We now turn to demonstrating the effectiveness of the feedback control design method using Green's function to create two nodes in a vibrating beam using two control forces receiving displacement and velocity measurements from sensors that are either collocated or noncollocated with the control actuator. Figure 12 shows the steady-state deflection of a damped cantilever beam with a concentrated harmonic force applied at $x_f = 1$ with frequency $\omega = 22$. The external damping coefficient $c_1 = 0.1$, while the internal damping coefficient $c_2 = 0.001$. It is desired to introduce two nodes at locations $x_{n_1} = 0.3$ and $x_{n_2} = 0.8$. To accomplish this task, two control forces with collocated sensors are applied at $x_{a_1} = 0.6$ and $x_{a_2} = 0.9$ with calculated displacement and velocity feedback gains $\alpha_1 = -1577.876$ and $\alpha_2 = -1.515$ for the first control force and $\alpha_3 = -2374.132$ and $\alpha_4 = -2.192$ for the second control force. The corresponding amplitudes of the control forces are $|u_1| = 1.463$ and $|u_2| = 0.396$. If, in certain applications, one wishes to place the actuators at the required nodes locations, i.e., $x_{a_1} = x_{n_1}$ and $x_{a_2} = x_{n_2}$, then the sensors should be placed at locations x_{s_1} and x_{s_2} different from the actuators locations x_{a_1} or x_{a_2}. This situation is illustrated in Figure 13, in which a simply supported beam is excited by a concentrated harmonic force that acts at $x_f = 0.5$ with the excitation frequency $\omega = 10$, which is very close to the beam nondimensional first natural frequency (π^2). It is required to create two nodes at $x_{n_1} = 0.6$ and $x_{n_2} = 0.8$ using two control forces with actuators located at the same locations as the nodes, i.e., $x_{a_1} = 0.6$ and $x_{a_2} = 0.8$. The two sensors, feeding back displacement signals to the two control force actuators,

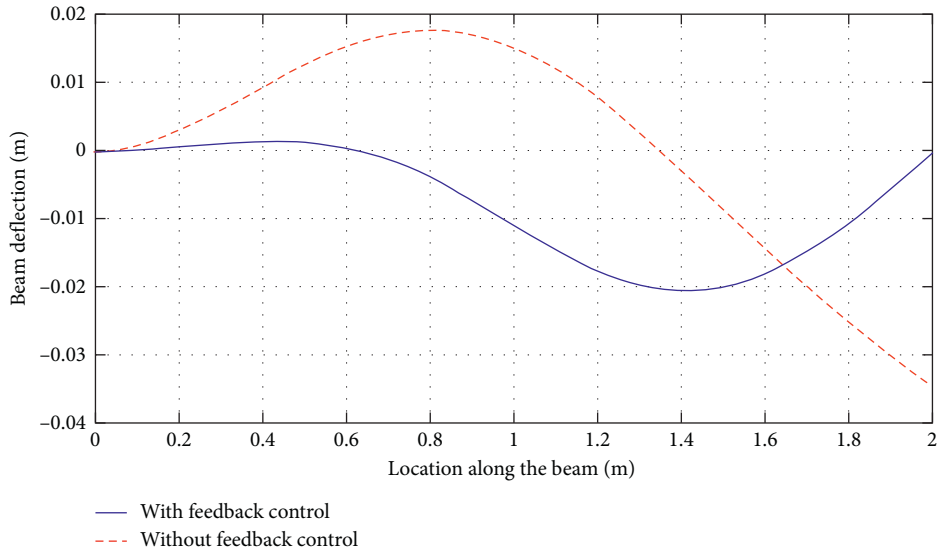

FIGURE 11: The steady-state deformed shape of a collocated controlled (solid line) and uncontrolled (dashed line) undamped cantilever beam when $\omega = 30.984$, $x_f = 1$, $x_n = 1$, and $x_a = 0.375$.

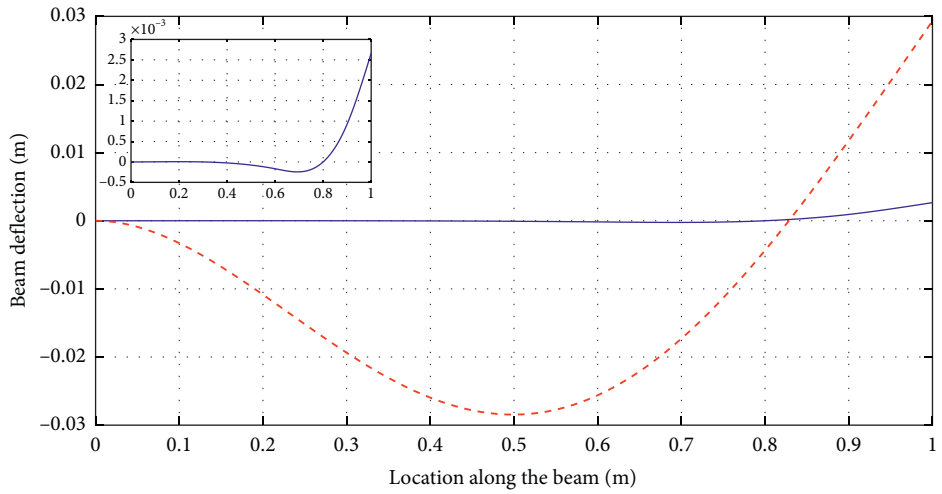

FIGURE 12: The steady-state deformed shape of a collocated controlled (solid line) and uncontrolled (dashed line) damped cantilever beam when $c_1 = 0.1$, $c_2 = 0.001$, $\omega = 22$, $x_f = 1$, $x_{n_1} = 0.3$, $x_{n_2} = 0.8$, $x_{a_1} = 0.6$, and $x_{a_2} = 0.9$. The inset shows the detailed plot of the controlled shape.

are located at $x_{s_1} = 0.4$ and $x_{s_2} = 0.7$. The required control gains are $\alpha_1 = -1579.109$ and $\alpha_2 = 0$ for the first control force and $\alpha_3 = -3999.314$ and $\alpha_4 = 0$ for the second control force, and the corresponding control force amplitudes are $|u_1| = 3.445 \times 10^{-11}$ and $|u_2| = 1.915 \times 10^{-10}$.

5.3. One Node with Zero Slope. In this section, numerical experiments are carried out to illustrate the applicability of the approach in Section 2.3 to impose a single node with both zero deflections and slopes using two control forces. While the zero deflections force a point on the beam to be stationary, the zero slopes create a flat region near the node having zero deflections, which makes the control design more robust.

Figure 14 displays the steady-state displacement of a controlled (solid line) and uncontrolled (dashed line) damped cantilever beam excited by a harmonic concentrated force applied at $x_f = 1$ with a frequency $\omega = 20$. It is desired to impose a node, having both zero deflections and slopes, at the beam location $x_n = 0.3$, using two collocated control forces applied at $x_{a_1} = 0.95$ and $x_{a_2} = 0.9$. The external and internal damping coefficients for the beam are $c_1 = 0.1$ and $c_2 = 0.001$, respectively. The calculated control gains are $\alpha_1 = -3.444 \times 10^{15}$ and $\alpha_2 = -7.066 \times 10^{13}$ for the first control force and $\alpha_3 = -96029.714$ and $\alpha_4 = -95.993$ for the second control force. The corresponding amplitudes of the two control forces are $|u_1| = 1.022$ and $|u_2| = 1.884$. As seen in the figure, the beam with control forces has a node exactly at $x_n = 0.3$ in addition to creating flat region having zero deflections over the whole beam span. Moreover, the controlled beam experiences vibrational amplitudes far less than the uncontrolled one compared to its uncontrolled counterpart. To demonstrate the noncollocated feedback control

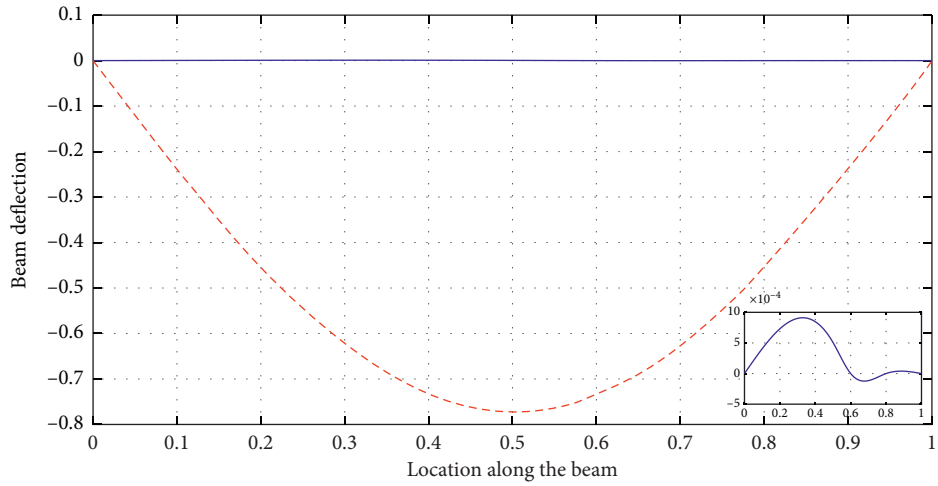

FIGURE 13: The steady-state deformed shape of a noncollocated controlled (solid line) and uncontrolled (dashed line) undamped simply supported beam when $\omega = 10$, $x_f = 0.5$, $x_{n_1} = 0.6$, $x_{n_2} = 0.8$, $x_{a_1} = 0.6$, $x_{a_2} = 0.8$, $x_{s_1} = 0.4$, and $x_{s_2} = 0.7$. The inset shows the detailed plot of the controlled shape.

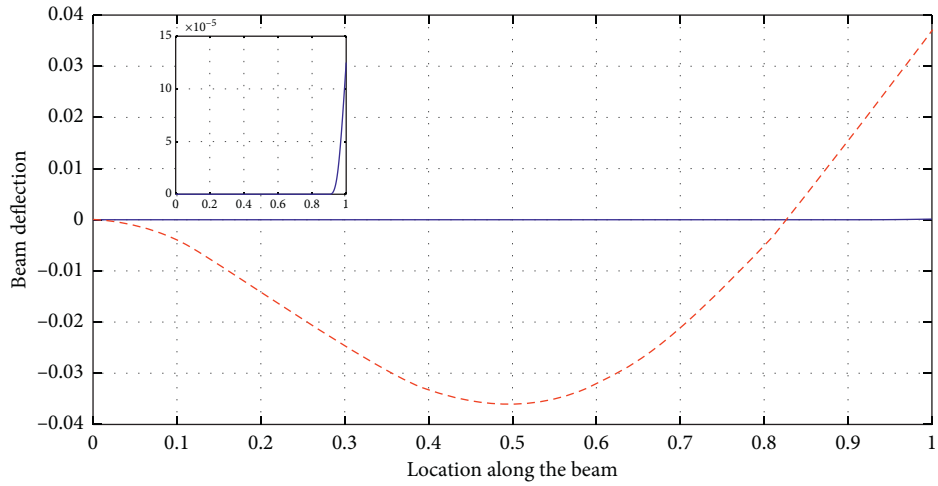

FIGURE 14: The steady-state deformed shape of a collocated controlled (solid line) and uncontrolled (dashed line) damped cantilever beam when $c_1 = 0.1$, $c_2 = 0.001$, $\omega = 20$, $x_f = 1$, $x_n = 0.3$, $x_{a_1} = 0.95$, and $x_{a_2} = 0.9$. The inset shows the detailed plot of the controlled shape.

case, it is assumed that a node is required to be enforced at the control force actuator location. In this case, the sensor for that actuator should be placed at any other different location from that of the actuator. This situation is illustrated in Figure 15, in which an undamped simply supported beam is excited by a concentrated harmonic force that acts at $x_f = 0.5$ with excitation frequency $\omega = 10$, which is very close to the beam nondimensional first natural frequency (π^2). It is required to create a node at the excitation force location, $x_n = 0.5$, having both zero deflections and zero slopes using two control forces. The solid curve corresponds to the deflected shape of the beam with two control forces acting at locations $x_{a_1} = 0.3$ and $x_{a_2} = 0.4$. The two sensors, feeding back displacement signals to the two control force actuators, are placed at the locations $x_{s_1} = 0.6$ and $x_{s_2} = 0.7$. The required control gains are $\alpha_1 = -5.630 \times 10^{15}$ and $\alpha_2 = 0$ for the first control force and $\alpha_3 = -7.587 \times 10^{15}$ and $\alpha_4 = 0$ for the second control force, and the corresponding control force amplitudes are $|u_1| = 4.831 \times 10^{12}$ and $|u_2| = 1.264 \times 10^{12}$. The dashed curve corresponds to the deflected shape of the beam with no control forces. This figure indicates that the controlled beam is practically motionless.

To show the computational efficiency of the proposed numerical method, an example reported in Cha and Zhou [27] is solved using the proposed numerical method. In Section 3.2 of their paper, they consider an undamped simply supported beam excited by a concentrated harmonic force with frequency $\omega = 57$ and an excitation location $x_f = 0.77$. Their goal is to impose a node with zero slopes at $x_n = 0.31$ using tuned translational and rotational oscillators attached to the beam at $x_a = 0.65$. All the previous parameters are nondimensional. They have shown the simulation of the steady-state lateral displacement of the beam in Figure 7 of their paper. The simulation contains three curves: the solid line corresponds to the deformed beam with sprung mass and rotational oscillator, the dashed dotted line

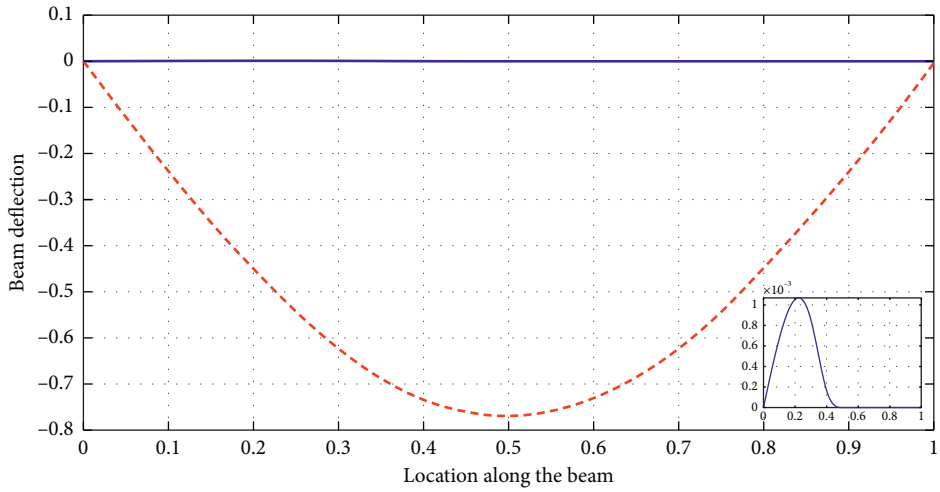

Figure 15: The steady-state deformed shape of a noncollocated controlled (solid line) and uncontrolled (dashed line) undamped simply supported beam when $\omega = 10$, $x_f = 0.5$, $x_n = 0.5$, $x_{a_1} = 0.3$, $x_{a_2} = 0.4$, $x_{s_1} = 0.6$, and $x_{s_2} = 0.7$. The inset shows the detailed plot of the controlled shape.

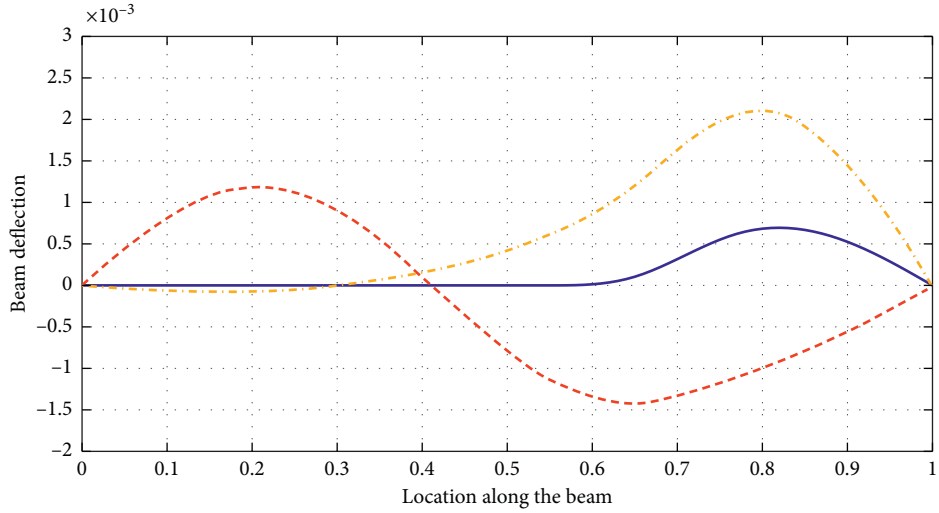

Figure 16: The steady-state deformed shape of a collocated controlled beam deflection having a node with zero slopes (solid line), a node (dashed dotted line), and uncontrolled beam deflection (dashed line) for the undamped simply supported beam when $\omega = 57$, $x_f = 0.77$, $x_n = 0.31$, $x_{a_1} = 0.65$, and $x_{a_2} = 0.55$.

corresponds to the deformed beam with sprung mass only, and the dashed line corresponds to the deformed beam without any oscillator. To simulate this problem, they have used 1000 terms in the assumed modes method and have to solve highly nonlinear simultaneous equations using the Matlab routine "fsolve" to search for a solution.

The same example is solved using the exact analytical solution outlined in Section 2.3 to impose a node with zero displacements and zero slopes using collocated feedback control case, with $x_{a_1} = 0.65$ and $x_{a_2} = 0.55$. First, equations (33a) and (33b) are solved for B and C, and then the feedback control gains are calculated using equations (31a) and (31b). The computations are performed using Matlab, and the execution time is about 2 seconds. The calculated displacement control gains for the two control forces that are responsible for imposing a node with zero slopes are -1.658×10^4 and -7.621×10^{14}, whereas that for imposing a node is -1.899×10^3. The steady-state responses for this case are shown in Figure 16. For comparison, the figure has three curves: the solid line corresponds to the deformed beam having a node with zero slopes, the dashed dotted line corresponds to the deformed beam having one node, and the dashed line corresponds to the deformed beam without feedback control. The two figures are comparable.

The formulation presented in this paper is applicable to any beam structure under conventional and non-conventional boundary conditions. This is due to the fact that Green's function derivation for a specific beam includes its boundary conditions, and, therefore, they are embedded in the derived Green's function for a specific beam. Therefore, the proposed feedback control design method is demonstrated only for cantilever and simply supported

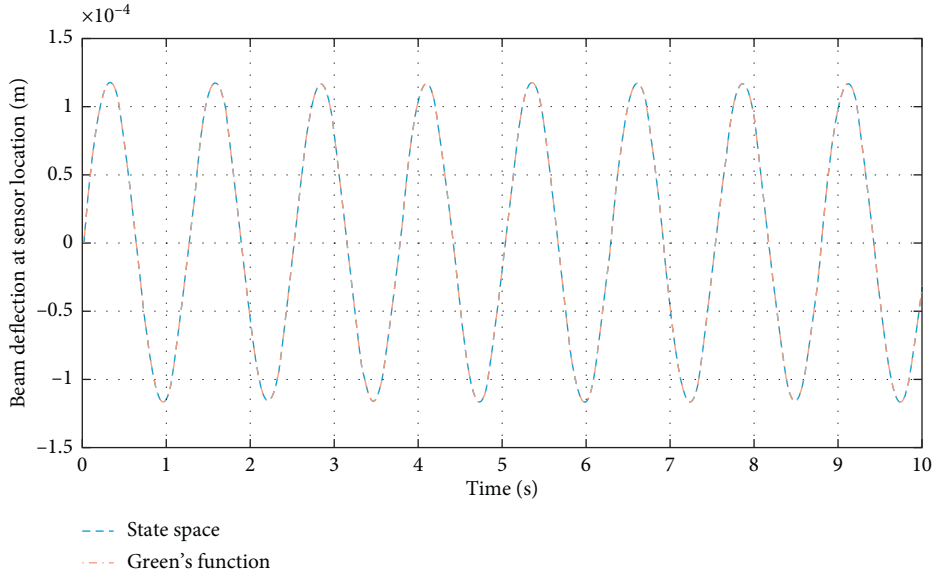

Figure 17: Beam deflection at sensor location ($w(x_s, t)$) simulated using Green's function and state-space models.

beams in the previous examples, and other types of beams are not considered for the sake of brevity.

5.4. Sensor Noise Simulation. The simulation of the procedure outlined in Section 4 is demonstrated on a damped cantilever beam system having a mass per unit length of 1 kg/m, flexural rigidity of 5 N·m^2, and length of 1 m. The beam is excited by a sinusoidal input of $\sin(\omega t)$ with frequency equals to 5 rad/s. It is desired to impose a node at location of 0.9 m using a control force with a collocated actuator and sensor at 0.95 m. The coefficients of external and internal damping are 0.1 N·s/m^2 and 0.001 N·s·m^2, respectively. The calculated displacement and velocity control gains are −9216.167 N/m and −2.229 N·s/m, respectively.

The state-space model outlined in Sections 3 and 4 is developed in Matlab using $n = 30$ states that represent the generalized coordinates $\eta_i(t), i = 1, 2, \ldots, 30$. The calculated state matrix and input matrix have sizes of 60×60 and 60×1, respectively. The output variable ($y(t)$), considered in this example, is the beam deflection at the sensor location ($w(x_s, t)$) so that the 1×60 output matrix and the feedforward matrices are given in equation (49).

To verify the accuracy of the state-space model, the beam deflection at the sensor location is calculated using Green's function and compared with that obtained using the state-space model and is shown in Figure 17. This figure shows an exact agreement for the beam deflection obtained by the two methods, which ensure the accuracy of the state-space model.

The sensor noise effect on the feedback control design using the state-space model is simulated using the Simulink block diagram shown in Figure 18. The sinusoidal excitation force with amplitude one and frequency 5 rad/s is generated by the sine wave block. To simulate a sensor noise, a random noise signal with the Gaussian distribution having a mean of zero and variance of 0.1 is created by the random source block. Both signals are added to form the input u^* to the state-space model. The state-space block contains the state, input, output, and feedforward matrices derived based on the aforementioned parameters having 30 states. The sensor noise filter transfer function, in equation (50), is represented by the low-pass filter block having a cutoff frequency equal to 10 rad/s.

The noisy excitation force input to the beam system represented by the state-space model is shown in Figure 19, while the unfiltered controlled beam deflection at the sensor location represented by the output of the state-space model is shown in Figure 20. The filtered sensor output represented by the output of the low-pass filter is shown in Figure 21. The low-pass filter is capable of eliminating the effect of noise on the sensor output as evidenced by comparing Figures 20 and 21.

6. Conclusions

In this paper, a numerical method is developed to eliminate the steady-state vibrations at a prescribed point or points in a harmonically vibrating structure. These points having zero displacements and/or zero slopes are referred to as nodes. The paper makes use of the dynamic Green's function to analyze the problem. The approach retains the infinite-dimensional model for the structure to derive the exact solution for the steady-state deflection in terms of algebraic equations. Therefore, the method is free from numerical inaccuracy when compared with modal superposition techniques. The main advantages of this approach are its generality and its computational simplicity. The nodes are created by applying feedback control forces. These control forces are constructed from displacement and/or velocity measurements using sensors located either at the control force position or at some other points. It is shown that if the system is damped, then the control force is proportional to the displacement and velocity, whereas it is proportional to the displacement only if the system is undamped. A closed form expression for the control gain(s) for three cases is

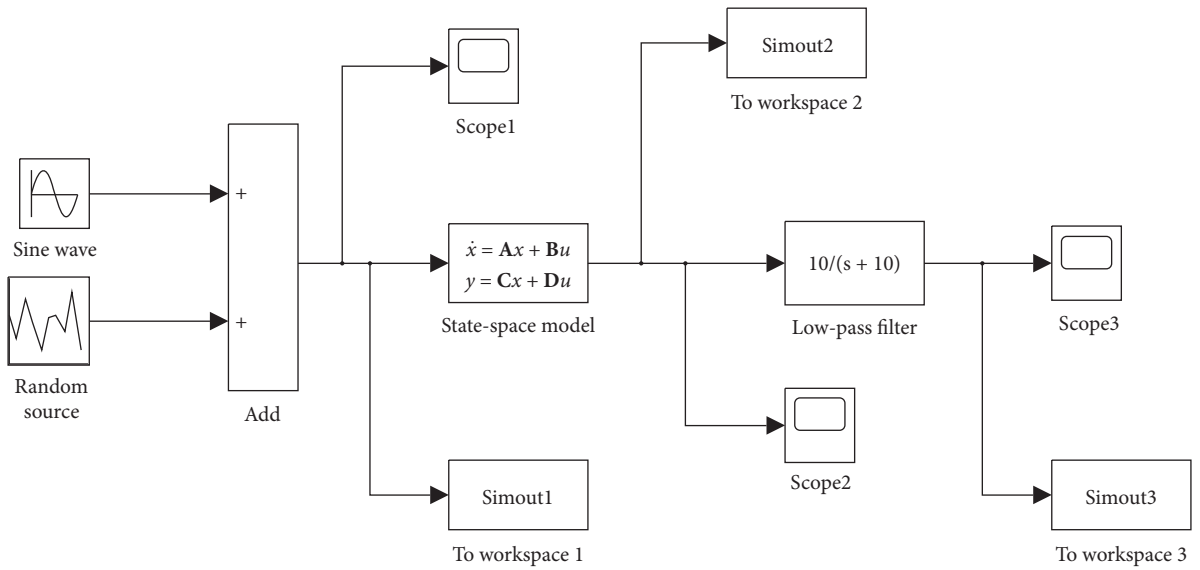

Figure 18: Simulink block diagram for the beam system model with sensor noise filter.

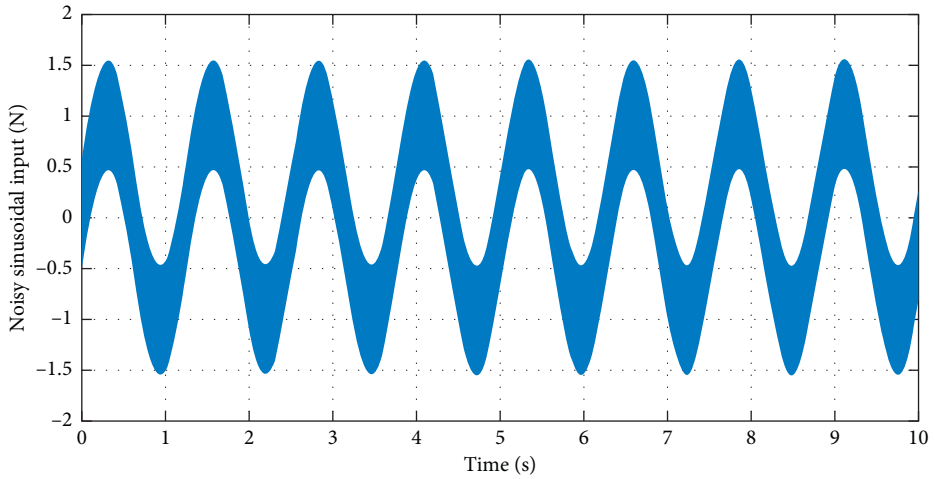

Figure 19: Noisy sinusoidal excitation force input $u^*(t)$.

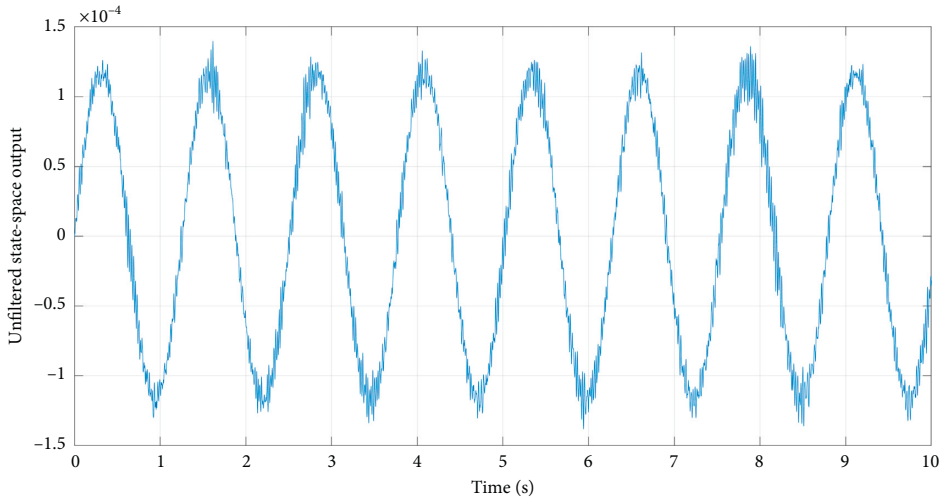

Figure 20: Unfiltered beam deflection at sensor location $(w(x_s, t))$.

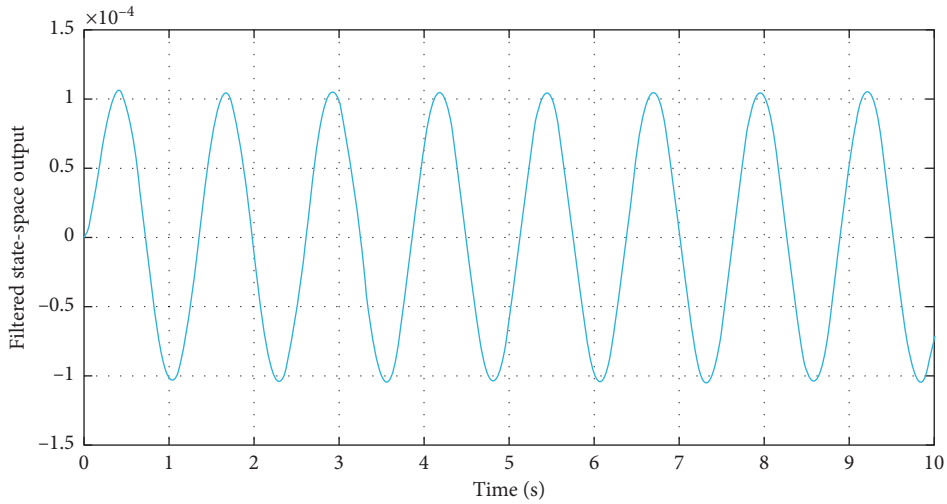

Figure 21: Filtered beam deflection at sensor location ($w(x_s, t)$).

presented by utilizing dynamic Green's function. These cases are creating one node, two nodes, and one node with zero slope at desired location(s) in a beam. The condition to create the node(s) using active or passive control is established. Several numerical examples are presented that show the effectiveness of the proposed control method. In the examples, it was shown that when the beam is excited near one of its natural frequency, then the feedback control force to create one node can lead to a motionless controlled beam. This is due to the fact that only one mode dominates the flexural wave contributing to the beam deformation and the control force creates antiwave that cancels the original flexural wave. Furthermore, when the locations of the two nodes are closely spaced, a motionless region on the beam can be created.

The stability of the feedback control system can be guaranteed provided that the gain of the control force satisfies a stability condition (34) for the undamped system. The stability of the damped beam system has been examined using the eigenvalues of the system matrix. Furthermore, a sensor noise rejection model is implemented using a first-order filter and its effect on the response of the feedback control system is demonstrated using a Simulink block diagram.

Data Availability

The data used to support the findings of this study are available from the corresponding author upon request.

Conflicts of Interest

The author declares that there are no conflicts of interest regarding the publication of this paper.

Acknowledgments

The author would like to acknowledge the support provided by the Deanship of Scientific Research at King Saud University through the Research Center at the College of Engineering.

References

[1] H. Frham, "Devices for damping vibration of bodies," US Patent No. 989958, 1911.

[2] J. Ormondroyd and J. P. Den Hartog, "The theory of dynamic vibration absorbers," *Transactions of the ASME*, vol. 50, pp. 9–22, 1928.

[3] J. E. Brock, "Damped vibration absorber," *Transactions of the American Society of Mechanical Engineers, Journal of Applied Mechanics*, vol. 68, p. A248, 1946.

[4] J. P. Den Hartog, *Mechanical Vibrations*, McGraw Hill, New York, NY, USA, 4th edition, 1956.

[5] J. B. Hunt, *Dynamic Vibration Absorbers*, Mechanical Engineering Publications Ltd., London, UK, 1979.

[6] B. G. Korenev and L. M. Reznikov, *Dynamic Vibration Absorbers: Theory and Technical Applications*, John Wiely, New York, NY, USA, 1993.

[7] J. Q. Sun, M. Jolly, and M. Norris, "Passive, adaptive and active tuned vibration absorbers—a survey," *Journal of Vibration and Acoustics*, vol. 117, pp. 234–242, 1999.

[8] A. H. von Flotow, A. Beard, and D. Bailey, "Adaptive tuned vibration absorbers: tuning laws, tracking agility, sizing, and physical implementations," in *Proceedings of National Conference on Noise Control Engineering (Noise-Con 94)*, pp. 437–454, Fort Lauderdale, FL, USA, May 1994.

[9] D. Young, "Theory of dynamic vibration absorbers for beam," in *Proceedings of the First U.S. National Congress of Applied Mechanics*, pp. 91–96, New York, NY, USA, 1952.

[10] J. C. Snowdon, "Steady-state behavior of the dynamic absorber," *Journal of the Acoustical Society of America*, vol. 31, no. 8, pp. 1096–1103, 1959.

[11] R. G. Jacquot, "Optimal dynamic vibration absorbers for general beam systems," *Journal of Sound and Vibration*, vol. 60, no. 4, pp. 535–542, 1978.

[12] H. N. Özgüven and B. Çandir, "Suppressing the first and second resonances of beams by dynamic vibration absorbers," *Journal of Sound and Vibration*, vol. 111, no. 3, pp. 377–390, 1986.

[13] D. N. Manikanahally and M. J. Crocker, "Experimental investigation of minimization of the dynamic response of mass-loaded beams using vibration absorbers," *Journal of the Acoustical Society of America*, vol. 93, no. 4, pp. 1896–1907, 1993.

[14] N. P. William, L. S. Ronald, and Q. He, "Controlled semiactive hydraulic vibration absorber for bridges," *Journal of Structural Engineering*, vol. 122, no. 2, pp. 187–192, 1996.

[15] G. J. Lee-Gulauser, G. Ahmedi, and L. G. Horta, "Integrated passive/active vibration absorber for multistory buildings," *Journal Structural Engineering*, vol. 123, no. 4, pp. 499–504, 1997.

[16] K. Nagaya, A. Kurusu, S. Ikai, and Y. Shitani, "Vibration control of a structure by using a tunable absorber and an optimal vibration absorber under auto-tuning control," *Journal of Sound and Vibration*, vol. 228, no. 4, pp. 773–792, 1999.

[17] P. D. Cha, "Natural frequencies of a linear elastica carrying any number of sprung masses," *Journal of Sound and Vibration*, vol. 247, no. 1, pp. 185–194, 2001.

[18] K. H. Low, "Frequencies of beams carrying multiple masses: Rayleigh estimation versus eigenanalysis solutions," *Journal of Sound and Vibration*, vol. 268, no. 4, pp. 843–853, 2003.

[19] J. R. Banerjee and A. J. Sobey, "Further investigation into eigenfrequencies of a two-part beam-mass system," *Journal of Sound and Vibration*, vol. 265, no. 4, pp. 899–908, 2003.

[20] J.-S. Wu and H.-M. Chou, "A new approach for determining the natural frequencies and mode shapes of a uniform beam carrying any number of sprung masses," *Journal of Sound and Vibration*, vol. 220, no. 3, pp. 451–468, 1999.

[21] J. H. Ginsberg, *Mechanical and Structural Vibrations: Theory and Applications*, John Wiley and Sons, New York, NY, USA, 2001.

[22] P. D. Cha and G. Ren, "Inverse problem of imposing nodes to suppress vibration for a structure subjected to multiple harmonic excitations," *Journal of Sound and Vibration*, vol. 290, no. 1-2, pp. 425–447, 2006.

[23] P. D. Cha and W. C. Wong, "A novel approach to determine the frequency equations of combined dynamical systems," *Journal of Sound and Vibration*, vol. 219, no. 4, pp. 689–706, 1999.

[24] P. D. Cha, "Imposing nodes at arbitrary locations for general elastic structures during harmonic excitations," *Journal of Sound and Vibration*, vol. 272, no. 3–5, pp. 853–868, 2004.

[25] K. Alsaif and M. A. Foda, "Vibration suppression of a beam structure by intermediate masses and springs," *Journal of Sound and Vibration*, vol. 256, no. 4, pp. 629–645, 2002.

[26] M. A. Foda and B. A. Albassam, "Vibration confinement in a general beam structure during harmonic excitations," *Journal of Sound and Vibration*, vol. 295, no. 3–5, pp. 491–517, 2006.

[27] P. D. Cha and X. Zhou, "Imposing points of zero displacements and zero slopes along any linear structure during harmonic excitations," *Journal of Sound and Vibration*, vol. 297, no. 1-2, pp. 55–71, 2006.

[28] P. D. Cha and C.-Y. Chen, "Quenching vibration along a harmonically excited linear structure using lumped masses," *Journal of Vibration and Control*, vol. 17, no. 4, pp. 527–539, 2010.

[29] Y. M. Ram, "Nodal control of a vibrating rod," *Mechanical Systems and Signal Processing*, vol. 16, no. 1, pp. 69–81, 2002.

[30] S. Elhay, G. M. L. Gladwell, G. H. Golub, and Y. M. Ram, "On some eigenvector-eigenvalue relations," *SIAM Journal on Matrix Analysis and Applications*, vol. 20, no. 3, pp. 563–574, 1999.

[31] A. N. Singh and Y. M. Ram, "Dynamic absorption in a vibrating beam," in *Proceedings of the Institution of Mechanical Engineers, Part C: Journal of Mechanical Engineering Science*, vol. 217, no. 2, pp. 187–197, 2006.

[32] N. Alujevic, I. Tomac, and P. Gardonio, "Tunable vibration absorber using acceleration and displacement feedback," *Journal of Sound and Vibration*, vol. 331, no. 12, pp. 2713–2728, 2012.

[33] M. A. Foda and K. Alsaif, "Control of lateral vibrations and slopes at desired locations along vibrating beams," *Journal of Vibration and Control*, vol. 15, no. 11, pp. 1649–1678, 2009.

[34] M. Abu-Hilal, "Forced vibration of Euler-Bernoulli beams by means of dynamic Green functions," *Journal of Sound and Vibration*, vol. 267, no. 2, pp. 191–207, 2003.

[35] G. F. Roach, *Green's Functions: Introductory Theory with Applications*, Van Nostrand Reinhold Company, London, UK, 1970.

[36] G. F. Roach, *Greens Functions*, Cambridge University Press, Cambridge, UK, 1982.